Research Square

Preprints are preliminary reports that have not undergone peer review.
They should not be considered conclusive, used to inform clinical practice,
or referenced by the media as validated information.

Parallel gas chromatography and photoacoustic spectroscopy for quantifying ethylene responses to nine modulating compounds in Arabidopsis and wheat

Jan Strnad
Laboratory of Growth Regulators, Faculty of Science, Palacký University
Michal Karady
michal.karady@upol.cz

Laboratory of Growth Regulators, Faculty of Science, Palacký University
Kateřina Cermanová
Laboratory of Growth Regulators, Faculty of Science, Palacký University
Jaromír Mikulík
Laboratory of Growth Regulators, Faculty of Science, Palacký University
Miroslav Strnad
Laboratory of Growth Regulators, Faculty of Science, Palacký University

Method Article

Keywords: Ethylene biosynthesis, gas chromatography, photoacoustic spectroscopy, Arabidopsis, wheat, 1-aminocyclopropane-1-carboxylic acid, ethylene inhibitors, phytohormones, ethephon, thidiazuron

Posted Date: November 11th, 2026

DOI: https://doi.org/10.21203/rs.3.rs-11477520/v1

License: This work is licensed under a Creative Commons Attribution 4.0 International License.
Read Full License

Additional Declarations: No competing interests reported.

Abstract

Background

Ethylene is a gaseous plant hormone controlling development, stress responses, and senescence, yet its quantitative measurement remains methodologically heterogeneous across plant research. Here, we present a unified experimental workflow that combines gas chromatography with flame ionization detection (GC–FID) and laser-based photoacoustic spectroscopy (PAS) for the quantification of endogenous ethylene production in plants. Although both techniques are widely used, a direct experimental comparison using identical biological samples has not been reported previously.

Results

Using *Arabidopsis* seedlings and wheat leaf segments, we demonstrate that GC–FID and PAS values are offset by a system-dependent proportional factor while following highly consistent dose-response trends across a broad range of ethylene-modulating treatments. Across all compounds and concentrations, ethylene values measured by both methods were strongly correlated. GC–FID provided superior linearity at high ethylene outputs, whereas PAS offered high sensitivity for low-to-moderate ethylene levels and faster sample throughput. The workflow defines a consistent set of experimental parameters, including delayed treatment application, normalization of ethylene production to plant fresh weight (FW), and minimization of biomass-related artefacts. Applying this approach, we systematically evaluated inhibitors and inducers of ethylene biosynthesis and signaling, including aminoethoxyvinylglycine (AVG), aminooxyacetic acid (AOA), 2-aminoisobutyric acid (AIB), 2-picolinic acid (2-PA), 1-aminocyclopropane-1-carboxylic acid (ACC), silver thiosulfate (STS), thidiazuron (TDZ), ethephon (ETH), and mebendazole (MEB). The data reveal pronounced species-specific sensitivities and clear toxicity thresholds for several compounds. Importantly, the parallel ethylene measurement workflow is compatible with downstream LC–MS/MS based phytohormone profiling. Correlation analysis of ethylene, its precursor ACC, multiple phytohormones, and FW is consistent with ACC availability as a significant determinant of ethylene production in Arabidopsis and wheat, while many apparent hormonal associations reflect indirect stress or growth effects rather than direct regulatory coupling.

Conclusion

This study provides a robust and extensible platform for ethylene quantification and interpretation across plant systems. The parallel GC–FID/PAS approach improves cross-validation of measurements and enables direct integration of ethylene production into broader phytohormonal analyses, facilitating reliable comparison of ethylene-related studies across laboratories and plant species.

Background

Ethylene functions as a plant hormone that modulates numerous aspects of plant growth, development, and stress responses, including seed germination, senescence, fruit ripening and abscission. Although it is not essential for viability — plants with diminished ethylene biosynthesis remain capable of completing their life cycle [1, 2] — it exerts strong regulatory influence over responses to abiotic and biotic stimuli. Due to its volatile nature and low endogenous concentrations, accurate quantification of ethylene production represents a persistent methodological challenge in plant research. Over the past decades, a variety of analytical techniques and principles have been developed to detect ethylene in gaseous mixtures, including gas chromatography (GC), photoacoustic spectroscopy (PAS), electrochemical sensors, optical spectroscopy-based approaches, resonance methods, and dielectric sensors [3,4].

Gas chromatography remains the most widely used and established method for ethylene quantification in laboratory plant biology. Since its introduction into plant research in the early 1960s [5], GC-based approaches—particularly GC coupled with flame ionization detection (GC–FID)—have become the benchmark for robustness, and broad dynamic range [3, 4]. GC methods are well suited for batch analysis of headspace samples and provide high analytical stability across long experimental series. However, GC-based ethylene measurements are limited by relatively long analysis times, lack of real-time monitoring, and high instrumentation costs. Portable micro-GC (μGC) systems enable field applications but generally suffer from substantially lower sensitivity and analytical performance compared with laboratory GC instruments [6].

Photoacoustic detection represents a complementary approach that has also been firmly established in plant ethylene research. PAS is an optical method based on infrared absorption and conversion of absorbed energy into an acoustic signal. Laser-driven photoacoustic detection was first introduced into plant physiology in the late 1980s [7] and has recently gained renewed attention due to the commercial availability of robust instruments such as the ETD-300 detector [8]. These systems provide high sensitivity, reliability, and flexibility, including real time measurements in continuous-flow mode [9, 10]. PAS systems are well suited for rapid or continuous measurements, although they are comparatively bulky and can be sensitive to environmental noise and vibration [6].

Despite frequent use of both GC-based and PAS-based methods in plant research, direct experimental comparisons between these technologies under identical biological and experimental conditions are lacking. Existing comparisons are generally theoretical or based on independent datasets obtained using different plant materials, experimental designs, or normalization strategies. To our knowledge, no study has directly quantified ethylene production from the same biological samples using both GC–FID and PAS. Moreover, integrated workflows combining both approaches within a single experimental pipeline remain rare in plant sciences. Similar multi-method approaches have been reported only sporadically in other research fields, such as the combination of GC and spectroscopic techniques for marine environmental analyses [11].

In parallel, recent studies demonstrate increasing use of PAS-based ethylene detectors for diverse biological questions, including ethylene receptor function and feedback regulation [12], light-regulated ethylene emission [13], and postharvest or stress-related responses. GC-based ethylene measurements are applied, for example in studies of wheat stress physiology [14]. This diversification makes cross-study comparability an increasingly practical concern. However, comparability is limited as much by biological variability as by instrumentation.

Experimental design varies considerably across the ethylene literature, which makes results difficult to compare. Reported protocols differ in the number of plants per sample vessel, the growth stage at treatment, the timing of ethylene accumulation, whether values are normalized to plant biomass, and whether seeds are germinated directly on treated media. Such factors can strongly influence measured ethylene output, particularly when a treatment affects plant growth or viability.

Methodological protocols for GC-based [15] and ETD-300 [9] measurements have been described previously. Here we build on these approaches by combining GC–FID and photoacoustic detection in a single workflow for measuring endogenous ethylene production, using identical biological samples to compare the two methods directly with respect to sensitivity, reproducibility, and biological interpretability. Alongside this comparison, we establish consistent conditions for several experimental parameters: FW normalization, treatment applied at a later developmental stage, and a reduced number of plants per vessel - to limit biomass-related variation, and we demonstrate that the same sample can subsequently be used for broader phytohormone profiling.

To assess the robustness and applicability of the workflow, we evaluated a panel of compounds known or proposed to influence ethylene biosynthesis, perception, or signaling [16, 17, 18, 19] in both *Arabidopsis thaliana* (L.) Heynh. seedlings and wheat (*Triticum aestivum* L.) leaf segments, representing dicotyledonous and monocotyledonous systems. We further demonstrate that the workflow is compatible with downstream phytohormone profiling by LC–MS/MS [20].

Materials and Methods

Ultrapure water (Milli-Q; Millipore, France) was used for the preparation of all solutions and media. Ethylene-modulating compounds and their suppliers are listed in Table 1. All other chemicals were of analytical or higher grade and, unless stated otherwise, were obtained from Merck (Merck KGaA, Darmstadt, Germany).

Arabidopsis growth conditions

Seeds of *A. thaliana* (Col-0) were sown in 20 mL transparent gas chromatography crimp vials (Agilent Technologies, USA) containing 4 mL of half-strength Murashige–Skoog medium (Apollo Scientific, United Kingdom), supplemented with MES (2-(N-Morpholino)ethanesulfonic acid) buffer (195 mg L^{-1}, pH 5.7; Serva, Germany), sucrose (10 g L^{-1}; Lach-Ner, Czech Republic), and agar (7 g L^{-1}; Duchefa, Netherlands). Twenty-five seeds were sown per vial.

Vials were sealed with parafilm and stratified for 2 days at 5°C. Plants were then grown in a controlled-environment growth chamber (Polyklima M4Z-TDL+; Polyklima, Germany) under a 16/8 h light/dark photoperiod at 23/18°C, white light intensity of 110–115 µmol m^{-2} s^{-1} with a 30-min ramp period, and 50% relative humidity.

After 7 days of growth, parafilm was removed and 100 µL of treatment solution was applied to the surface of the agar medium. Vials were gently tilted and rotated manually to ensure uniform distribution of the solution. Following 1 h of evaporation in a laminar flow hood, vials were gas-tight sealed with crimp caps and returned to the growth chamber for an additional 48 h. Control vials without plants (with medium) were treated identically using the highest concentration of each compound. Four replicate vials were prepared per treatment–dose combination. Ethylene measured in these vials was subtracted on both platforms.

Arabidopsis treatments

The following compounds were tested: 2-picolinic acid (2-PA), aminocyclopropane-1-carboxylic acid (ACC), silver thiosulfate (STS), 2-aminoisobutyric acid (AIB), aminooxyacetic acid (AOA), aminoethoxyvinylglycine (AVG), ethephon (ETH), mebendazole (MEB), and thidiazuron (TDZ). Suppliers and solvents are listed in Table 1.

All compounds were applied in 100 µL volumes at concentrations specified in Table 1, calculated relative to agar volume.

Table 1
Composition of solutions used to treat Arabidopsis plants

compound	supplier	concentrations relative to agar [μM]	concentrations of applied solution [mM]	solvent
2-PA	Sigma Aldrich, USA	**0; 50; 100; 500; 1 000; 5 000**	0; 2; 4; 20; 40; 200	water
ACC	Sigma Aldrich, USA	**0; 1; 5; 10; 50; 100**	0; 0.04; 0.2; 0.4; 2; 4	water
STS	prepared from silver nitrate (Alfa Aesar, USA) and sodium thiosulfate (Lach-Ner, Czech Republic)	**0; 1; 5; 10; 50; 100**	0; 0.04; 0.2; 0.4; 2; 4	water
AIB	Sigma Aldrich, USA	**0; 10; 50; 100; 500; 1 000**	0; 0.4; 2; 4; 20; 40	water
AOA	Sigma Aldrich, USA	**0; 100; 500; 1 000; 5 000; 10 000**	0; 4; 20; 40; 200; 400	water
AVG	OlChemIm, Czech Republic	**0; 0.05; 0.1; 0.5; 1; 5**	0; 0.002; 0.004; 0.02; 0.04; 0.2	water
ETH	Sigma Aldrich, USA	**0; 10; 50; 100; 500; 1 000**	0; 0.4; 2; 4; 20; 40	water
MEB	Sigma Aldrich, USA	**0; 0.5; 1; 5; 10; 50**	0; 0.02; 0.04; 0.2; 0.4; 2	water (suspension)
TDZ	OlChemIm, Czech Republic	**0; 0.5; 1; 5; 10; 50**	0; 0.02; 0.04; 0.2; 0.4; 2	0.7% DMSO

All compounds were applied as 100 μl of either solution in ultrapure water or when not applicable due to reduced solubility in 0.7% DMSO (dimethylsulfoxide, in ultrapure water; v/v) or as a suspension. The intended final concentration was relative to agar.

Wheat growth conditions

Wheat experiments were performed using spring wheat (*Triticum aestivum* L. cv. Aranka) and were adopted from the senescence bioassay described by Holub et al. [21]. Seeds were washed several times with water, soaked for 3 h, and sown on perlite saturated with Hoagland's solution (pH 5.8). Plants were grown in a growth chamber (Conviron GEN1000; Conviron, Canada) under a 16/8 h light/dark cycle at 23°C and light intensity of 50 μmol m^{-2} s^{-1}.

After 7 days, when the first leaf was fully expanded, tip segments (approximately 3.5 cm) from the first leaf were excised from ten seedlings and trimmed to a combined FW of 250 mg. The leaf segments were

placed into 20 mL crimp vials containing 1 mL of treatment solution. To remove ethylene released immediately after excision, samples were immediately flushed with compressed air in a separate room and left open for 30 min in a fume hood before sealing.

Sealed vials were incubated for 48 h under the same environmental conditions as Arabidopsis plants. Control vials without plant material contained the highest concentration of each respective treatment solution. Headspace ethylene was subsequently quantified as described below.

Because segments were trimmed to a fixed starting mass, absolute FW at harvest varied little between treatments (251–273 mg across the whole study). For wheat we therefore additionally report FW change over the 48 h incubation — mass gained relative to the 250 mg starting material — which is the biologically informative growth measure in this assay. Both absolute FW and FW change are given in Additional file 3. Ethylene normalization for wheat uses absolute harvest FW, as for Arabidopsis.

Wheat treatments

Wheat leaf segments were treated with the same panel of compounds as Arabidopsis, applied independently in aqueous solutions at concentrations specified in Table 2.

Table 2
Composition of solutions used to treat wheat leaves

compound	concentrations of applied solutions [µM]	solvent
2-PA	0; 50; 100; 500; 1 000; 5 000	water
ACC	0; 1; 5; 10; 50; 100	water
STS	0; 10; 50; 100; 500; 1 000	water
AIB	0; 100; 500; 1 000; 5 000; 10 000	water
AOA	0; 100; 500; 1 000; 5 000; 10 000	water
AVG	0; 1; 5; 10; 50; 100	water
ETH	0; 10; 50; 100; 500; 1 000	water
MEB	0; 0.5; 1; 5; 10; 50	water
TDZ	0; 0.5; 1; 5; 10; 50	water

All compounds were applied as 1 ml of solution into which the basal ends of leaf segments were immersed.

Ethylene measurements

Ethylene production was quantified using a unified workflow consisting of two consecutive analytical methods applied to the same sealed sample vessels. Headspace ethylene was first quantified by gas chromatography with flame ionization detection (GC–FID), followed by photoacoustic spectroscopy (PAS) using an ETD-300 detector.

Gas chromatography (GC–FID)

For GC analysis, 1 mL of headspace gas was withdrawn from each sample vial using an automated headspace sampler (Agilent G1888; Agilent Technologies, USA) and injected into a gas chromatograph (Agilent 6890N) equipped with a flame ionization detector. Separation was performed on an Agilent HP-PLOT Q column (Agilent Technologies, USA) shortened to 21 meters (530 µm diameter, 40 µm film thickness), operated isothermally at 50°C for 2 minutes, followed by 3 minute linear ramp to 110°C, followed by 2 minutes of isothermal operation followed by 1 minute conditioning to starting conditions. Total runtime of the analysis was 8 minutes. Nitrogen served as the carrier gas at a flow rate of 6 mL min^{-1}. The detector temperature was set to 250°C. Headspace sampler parameters were as follows: Vial equilibration 0.5 min, pressurization time 0.2 min, loop fill time 0.2 min, loop equilibration time 0.05 min, injection time 1 min, oven temperature 50°C, loop temperature 90°C, transfer line temperature 120°C. GC ChemStation Rev. B01.03 (build 204) (Agilent Technologies, USA) software was used to operate the instrument and evaluate data.

Photoacoustic spectroscopy (PAS)

Following GC analysis, the remaining headspace gas in the same vials was analyzed using a laser-based photoacoustic ethylene detector (ETD-300; Sensor Sense B.V., Nijmegen, Netherlands) equipped with a VC-6 valve controller (Sensor Sense B.V., Nijmegen Netherlands). Ambient air, supplied by an air pump and passed through hydrocarbon-removing catalytic filters, was used as the carrier gas. Sampling was performed via flushing the sealed vial headspace through inlet and outlet tubing system of VC-6. Valve Controller software version 1.4.3 (Sensor Sense B.V., Nijmegen, Netherlands) software was used to operate the instrument and evaluate data.

Measurements were conducted in “samples mode” according to the manufacturer’s terminology. Unless ethylene concentrations exceeding 2000 ppb (parts per billion (v/v)) were expected (based on prior GC measurements), detector sensitivity was set to “fine” mode. Air flow was maintained at 5 L h^{-1} with a sampling duration of 5 min per vial.

Sample processing and normalization

After completion of both ethylene measurements, vials were opened and plant material from each vial was removed and weighed collectively to determine FW. Samples were then immediately frozen in liquid nitrogen and stored at − 80°C for subsequent phytohormone analysis.

Ethylene values obtained by PAS were corrected for the 1 mL headspace volume removed during GC sampling. Headspace-sampler settings were identical for both plant systems. Final ethylene production rates were normalized to plant FW. Statistical evaluation was performed using Welch ANOVA followed by Dunnett's post-hoc test using Microsoft Excel with "Real Statistics Using Excel" add-in.

Headspace ethylene concentrations (ppb, v/v) were converted to absolute amounts using the ideal gas law, taking free headspace volume as the nominal vial volume minus the volume of medium and/or treatment solution, at incubation temperature and ambient pressure. Amounts were divided by sample FW and by the 48 hour accumulation period to give production rates in pmol·mg $(FW)^{-1}$·48 h^{-1}.

Analytical performance and calibration

Calibration curves for both analytical systems were generated using manually prepared ethylene–air mixtures derived from pure ethylene gas (Sigma-Aldrich, USA). Linear ranges and coefficients of determination are given

in Additional file 1. Accuracy of calibration curves was confirmed using calibrated ethylene (99 and 515 ppb) mixtures with nitrogen (SIAD, Italy).

LC–MS/MS of ACC and phytohormones

Following ethylene quantification and sample weighing, plant material was frozen and afterwards recovered from each vial and ground to a fine powder using zirconium oxide beads (Next Advance, USA) and a bead mill (MM 400; Retsch, Germany) at 27 Hz for 2 min. Ground material from the replicate vials of each treatment–dose combination was pooled, and five aliquots of 10 mg FW were taken from the pooled powder. Phytohormones and related compounds were extracted and quantified following the validated LC–MS/MS protocol of Karady *et al.* [20], using derivatization for ACC analysis [22]. Contents are expressed in pmol·g^{-1} FW. Values below the limit of quantification were reported as not determined. Data are given in Additional files 2 and 3.

Hormone concentrations were calculated using stable isotope-labelled internal standards and expressed relative to FW, corresponding to ethylene production normalization. Pearson correlation analyses were conducted to examine relationships between phytohormone levels, ethylene production measured by both GC–FID and PAS, plant FW, and applied treatment concentrations. Correlations were computed on treatment–dose means (n = 54 per species; 42 without the ACC and ETH series) and, for Figs. 6–7, within each compound series (six dose levels).

Measured phytohormone concentrations are provided in Additional files 2 and 3, and complete correlation matrices are presented in Additional files 10 and 11. Analyses were performed using Excel Professional Plus 2021 (Microsoft, Redmond, USA) with "Real Statistics Using Excel" add-in.

Results and discussion

Method comparison and analytical performance

Calibration experiments demonstrated that GC–FID exhibited the broadest dynamic range, with linear response extending from 27 ppb up to at least 2.06×10^6 ppb ethylene ($R^2 = 0.999985$). In contrast, the PAS detector ETD-300 operated in fine mode showed linearity between 5.64 and approximately 1.3×10^4 ppb ($R^2 = 0.999649$), while coarse mode extended the upper linear range to approximately 9.7×10^4 ppb ($R^2 = 0.999907$) but with reduced sensitivity at low concentrations (Additional file 1).

These differences were reflected in biological experiments. Low ethylene emissions typical of untreated controls or inhibitor-treated samples were reliably quantified by both GC–FID and PAS in fine mode. However, treatments inducing strong ethylene production (e.g. high-dose ACC or ETH) frequently exceeded the linear range of PAS “fine” mode, necessitating “coarse” mode operation. Further increases of ethylene production, especially in case of ethephon, would necessitate reliance on GC-FID.

While GC–FID required only a small headspace volume (1 mL), allowing potential repeated sampling, PAS operated as a flow-through system and therefore consumed the entire remaining vial headspace. Analysis times were 8 min for GC-FID and 5 min for PAS. Both methods could be operated faster, but at the cost of compromised baseline stability or increased interference from late-eluting impurities [23].

Across all treatments and concentrations in both plant species, ethylene values obtained by GC–FID and PAS were closely correlated within each plant system (pooled r = 0.995 in Arabidopsis, 1.000 in wheat), but their absolute values differ by a system-dependent factor (median GC–FID/PAS ratio 2.11 in Arabidopsis and 1.13 in wheat). In *A. thaliana*, Pearson correlation coefficients between GC–FID and PAS measurements consistently exceeded r = 0.97 across treatment series (Additional file 10), indicating excellent agreement between methods over the biologically relevant concentration range. Comparable correlations were observed in wheat leaf segments (Additional file 11), despite lower absolute ethylene production relative to Arabidopsis.

Thus, the two methods provided congruent relative trends across treatments, while GC–FID offered a wider linear range at high ethylene levels and PAS enabled rapid, high-throughput quantification of low to moderate ethylene production. Both analytical methods exhibited low technical variability, with relative standard deviations typically below 15% for biological replicates across all treatments. Variability largely reflected biological rather than analytical noise, especially in wheat, where wound responses and tissue heterogeneity contribute additional variance despite pre-incubation flushing.

Normalization, species differences and practical complementarity

Normalization to plant FW allowed effects on ethylene production to be distinguished from effects on plant growth. This was most relevant for compounds that inhibited growth at the concentrations tested. With AOA, ethylene output per vial in *Arabidopsis* changed little (57–91 vs 81 pmol per vial by PAS), whereas FW declined, so that FW-normalized production increased 2.7-fold (PAS) and 3.5-fold (GC–FID).

With 2-PA, FW-normalized production in *Arabidopsis* was 10–24% lower than in controls at 50–100 µM and higher at growth-inhibiting concentrations. In wheat it did not change up to 1 000 µM (Additional files 2, 3).

Absolute ethylene production differed substantially between Arabidopsis seedlings and wheat leaf segments. Arabidopsis produced ethylene levels exceeding several hundred pmol·mg(FW)$^{-1}$·48h^{-1} under strong inducers (e.g. ACC, ETH), whereas wheat leaf segments generally remained within the lower PAS detection range under comparable treatments.

As a result, PAS fine mode was sufficient for most wheat experiments without detector saturation, allowing rapid measurements with high sensitivity. In Arabidopsis, PAS remained highly suitable for inhibitor screening and low-dose inducer experiments, whereas GC–FID provided analytical headroom for strong induction treatments even when compared to PAS coarse mode. This complementarity highlights the benefit of combining both techniques within a single workflow.

Taken together, these data demonstrate that GC–FID and PAS are not competing but complementary approaches for ethylene quantification. PAS offers fast, sensitive, and non-destructive detection suited for high-throughput screening and physiological or low-ethylene samples, while GC–FID provides superior linearity over an exceptionally wide concentration range and robust quantification of high ethylene outputs.

The strong correlation between methods across two plant systems, combined with predictable deviations at known technical limits, validates their parallel use for reproducible and biologically interpretable ethylene measurements. Deviations observed at high ethylene concentrations were consistent with known dynamic range limitations of PAS fine mode and did not affect qualitative interpretation.

A major outcome of this study is that experimental normalization to FW and timing matter at least as much as analytical sensitivity: across several treatments, this normalization changed the interpretation outright, and no increase in detector performance would have compensated for its absence.

Treatments and ethylene production

Plant material and treatment

To ensure reliable and comparable quantification of endogenous ethylene production, experimental conditions were optimized to minimize biological variability while preserving sensitivity. Particular emphasis was placed on normalization to plant FW and on avoiding early developmental biases caused by germination on treated media.

Compared with previously published ethylene bioassays [24, 25], we used a reduced number of Arabidopsis plants (25 per vial). This number was sufficient to generate reliably measurable ethylene

levels while allowing uniform growth and accurate FW determination, yet still enabling enough plant material for subsequent downstream analyses.

Because of low germination uniformity and poor reproducibility associated with direct wheat sowing, a modified wheat leaf segment bioassay was employed, adapted from Holub et al. [21]. This approach provided a highly reproducible monocot system suitable for comparative ethylene measurements.

Building on established GC-based protocols [15], the combined use of delayed treatment application and FW normalization allowed ethylene output to be distinguished from changes in plant biomass.

To simulate treatment of established plants, seedlings were germinated on untreated medium and treated at a later developmental stage rather than germinated directly on treated media, which can itself influence plant mass. Plant weight is also a workable, if approximate, indicator of treatment toxicity. Growth and viability responses to the compound panel are summarised in Table 3. Only AOA and 2-PA reached doses that arrested growth in both species, and the interval between the lowest growth-inhibiting dose and the lethal dose was narrow — one order of magnitude for AOA in Arabidopsis (500 to 5 000 µM) and for 2-PA (500 to 5 000 µM) — so that in both cases the concentrations affecting ethylene output overlap those affecting viability. The remaining compounds were not deleterious at any dose tested (AVG, AIB, ACC, TDZ, MEB in both species) or affected growth only at the upper end of the range (STS and ETH in Arabidopsis).

Table 3
Overview of deduced treatment toxicity at the doses used to influence ethylene production.

plant	treatment	maximum dose	growth inhibiting dose	visual symptoms causing dose	lethal /growth stopping dose
Arabidopsis	**AVG**	5 μM	ND	ND	ND
	AOA	10 000 μM	≥ 500 μM	≥ 1 000 μM	≥ 5 000 μM
	2-PA	5 000 μM	≥ 500 μM	≥ 500 μM	5 000 μM
	AIB	1 000 μM	ND	ND	ND
	ACC	100 μM	ND	ND	ND
	ETH	1 000 μM	≥ 500 μM	ND	ND
	TDZ	50 μM	ND	ND	ND
	STS	100 μM	≥ 50 μM	ND	ND
	MEB	50 μM	ND	ND	ND
wheat	**AVG**	100 μM	ND	ND	ND
	AOA	10 000 μM	≥ 5 000 μM	≥ 5 000 μM	10 000 μM
	2-PA	5 000 μM	≥ 1 000 μM	≥ 1 000 μM	ND
	AIB	10 000 μM	ND	ND	ND
	ACC	100 μM	ND	ND	ND
	ETH	1 000 μM	ND	ND	ND
	TDZ	50 μM	ND	ND	ND
	STS	1 000 μM	ND	ND	ND
	MEB	50 μM	ND	ND	ND

Growth inhibiting dose – lowest doses at which statistically significant ($p < 0.05$) inhibition of growth was observed. Visual symptoms causing dose – lowest doses, at which observable discoloration occurred. Lethal/growth stopping dose – lowest doses completely lethal for Arabidopsis (all plants) or completely stopping wheat leaf segment growth. ND (not determined) – even the highest dose used did not cause indicated effect. For wheat, growth effects refer to FW gained during the 48 h incubation.

Inhibitors of ACC synthase

Aminoethoxyvinylglycine (AVG) treatment

AVG is a natural fermentation product and plant growth regulator that inhibits ethylene biosynthesis, commonly sold as ReTain ® or PinCor ®. It is used in agriculture to delay fruit ripening, increase firmness, reduce pre-harvest drop, and manage harvest timing in crops such as apples, pears, pineapples etc. [16, 26, 27].

AVG caused a clear, dose-dependent suppression of ethylene production in both species (Fig. 1). In Arabidopsis, suppression was statistically significant ($p < 0.05$, relative to control, as in all cases where statistical significance is mentioned onward) from 0.05–0.1 µM upward. FW was not significantly affected. At 1 µM AVG, Arabidopsis ethylene production per FW was reduced approximately 5.7-fold (from 1.64 to 0.29 pmol·mg^{-1}·48h^{-1} by PAS) or 3.4-fold (from 2.47 to 0.73 pmol·mg^{-1}·48h^{-1} by GC) relative to the control, plateauing at 5 µM on levels similar to 1 µM. Ethylene levels at 0.5–5 µM approached the lower quantifiable range of the GC, while PAS measurements remained well within its reliable detection range. Data are given in Additional file 2.

Phytohormonal analysis revealed decrease in ACC levels (from 675 to 181 pmol·g^{-1}) consistent with the role of AVG as an ACS (ACC synthase) modulator [16, 28, 29]. An increase in ABA (abscisic acid) that strongly correlated with the applied dose, together with noticeable shift of auxin content from conjugates into active free IAA (indole-3-acetic acid) form accompanied by increase in *t*Z (*trans*-zeatin) levels was also observed.

Wheat required approximately two orders of magnitude higher concentrations (≥ 50 µM) to show a similar effect as Arabidopsis (FW also not significantly affected). Significant suppression occurred at ≥ 50 µM, reaching 2.5-fold (from 0.61 to 0.24 pmol·mg^{-1}·48h^{-1} by PAS) or 2-fold (0.67 to 0.33 pmol·mg^{-1}·48h^{-1} by GC) reduction at 100 µM. Phytohormonal profiling also revealed decrease in ACC levels (from 840 to 207 pmol·g^{-1}), but the correlation was weaker than in case of Arabidopsis. The overall pleiotropic effects were generally also weaker. Data are provided in Additional file 3.

Dose–response analysis of ethylene biosynthesis inhibition by aminoethoxyvinylglycine (AVG) in *Arabidopsis thaliana* seedlings and wheat (*Triticum aestivum*) leaf segments. Headspace ethylene concentration after 48 h (ppb) in sealed sample vessels and plant fresh weight (FW) at harvest are shown in panels **A** (*A. thaliana*) and **C** (wheat). Ethylene production normalized to FW is shown in panels **B** (*A. thaliana*) and **D** (wheat). Measurements were performed after 48 h of treatment and incubation. Data are presented as means ± SD. Statistical significance relative to untreated controls is indicated by asterisks in the colour of the data series (Welch's ANOVA with Dunnett's test, $p < 0.05$); n = 3–4 independent biological replicates.

Aminooxyacetic acid (AOA)

AOA, a pyridoxal phosphate–dependent enzyme inhibitor commonly used to suppress ACC synthase activity [16, 30, 31], was included to compare its inhibitory efficiency and specificity with AVG and to further validate the ethylene measurement workflow.

In Arabidopsis seedlings, AOA did not cause any meaningful reduction of ethylene production across the entire tested concentration range by both GC–FID and PAS (Additional files 2 and 4). In contrast to AVG, AOA exhibited a slight increase in production, with absolute ethylene emission declining once concentrations exceeded 500 µM. At the highest concentrations tested (≥ 1 000 µM), absolute ethylene production returned to near-baseline levels, as consistently detected by both analytical techniques. However, unlike AVG, AOA treatment strongly negatively affected plant FW (from 45.70 mg to already 16.13 mg at 1 000 µM and lower at concentrations ≥ 1 000 µM). After normalization, production per plant FW mass increased because FW generally declined.

Phytohormonal profiling revealed a pronounced reduction in ACC levels with increasing AOA concentration (from 611 to 2 $pmol \cdot g^{-1}$), consistent with ACS inhibition, yet inconsistent with effects on ethylene biosynthesis. At the same time, broad alterations in phytohormone profiles were observed at higher AOA concentrations, including changes in auxins, salicylic acid, abscisic acid, and jasmonates (Additional file 2). These effects indicate that, in Arabidopsis, AOA exerts substantially less biochemical specificity than AVG and affects additional metabolic and phytohormonal pathways at higher doses.

In wheat leaf segments, AOA reduced ethylene production in a concentration-dependent manner and the overall response differed markedly from Arabidopsis (Additional file 3 and 4). Low to moderate AOA concentrations resulted in sharp reductions in ethylene emission (up to 3.4-fold (from 0.68 to 0.20 $pmol \cdot mg^{-1} \cdot 48h^{-1}$ by PAS) or 2.6-fold (from 0.73 to 0.28 $pmol \cdot mg^{-1} \cdot 48h^{-1}$ by GC)) at 500 µM, whereas concentrations higher than 1 000 µM led to partial recovery of ethylene production almost to the level of control. As in Arabidopsis, FW inhibitory effects became prominent with increasing AOA concentrations up to almost complete toxicity at 10 000 µM (decrease of FW gain from 13.75 to 1.85 mg).

Hormonal profiling of wheat leaf segments revealed decreases in ACC content (from 669 to 303 $pmol \cdot g^{-1}$) with increasing AOA concentration, consistent with inhibition of ethylene biosynthetic flux. In contrast to Arabidopsis, however, off-target hormonal disturbances were less pronounced in wheat, possibly reflecting reduced metabolic plasticity in excised leaf tissue (Additional file 3).

Inhibitors of ACC oxidase

2-Picolinic Acid (2-PA)

2-PA has been identified as an inhibitor of ACC oxidase (ACO) and has been used to infer causal roles of ethylene in plant responses [18]. Given reports of toxicity of its derivatives [32], 2-PA was included here to evaluate its specificity and suitability as an ethylene biosynthesis inhibitor under normalized measurement conditions.

In Arabidopsis seedlings, ethylene emission expressed per vial remained unchanged across a wide concentration range (50–1 000 µM), as consistently measured by both GC–FID and PAS (Fig. 2; Additional file 2). 2-PA caused a pronounced, concentration-dependent reduction in plant FW, already evident at 500 µM and becoming severe at higher concentrations (from 58.77 to 22.80 mg at 5 000 µM).

At the highest concentrations tested (≥ 500 µM), where FW was drastically reduced, normalized ethylene production increased, consistent with rather broader metabolic impairment than specific ACO inhibition. Plants exposed to 1 000 µM exhibited visible growth inhibition, and those treated with 5 000 µM showed complete loss of growth and pigmentation.

Phytohormonal profiling reveals that ACC levels increased markedly (from 744 up to 26 040 pmol·g^{-1} at 1 000 µM) with increasing 2-PA concentration, while ethylene output per vial remained unchanged or did not change proportionally to ACC levels, which is consistent with reduced conversion of ACC to ethylene [18]. In parallel, pronounced alterations in multiple hormone pathways were observed, including strong increases in stress-related hormones and disruptions of auxin and cytokinin homeostasis (Additional file 2). At the growth-inhibiting concentrations (≥ 500 µM), these hormonal changes accompanied the reduction in FW, indicating that effects on plant growth and hormone homeostasis contribute to the ethylene response observed at these doses.

In wheat leaf segments, 2-PA exhibited a different response pattern compared with Arabidopsis, highlighting the importance of species-specific validation (Fig. 2; Additional file 3). Over most of the concentration range tested (50–1 000 µM), normalized ethylene production in wheat was largely unaffected followed by a slight increase of ACC and visible growth-retardant effects with increasing concentrations. Only at the highest tested concentration (5 000 µM) did ethylene production increase noticeably (from 0.59 to 1.50 pmol·mg^{-1}·$48h^{-1}$ by PAS; from 0.65 to 1.70 pmol·mg^{-1}·$48h^{-1}$ by GC), coinciding with severe tissue damage and strong shifts in hormonal profiles, including extreme increases in ACC (from 813 to 13 915 pmol·g^{-1}), stress-associated hormones [JA, JA-Ile (jasmonic acid and its conjugate with isoleucine)] and auxin and cytokinin homeostasis. Unlike ethylene biosynthesis inhibitors such as AVG, 2-PA did not produce a coordinated decrease in ethylene emission and ACC content.

Figure 2. Effects of 2-PA on ethylene production in Arabidopsis and wheat.

Dose–response analysis of ethylene production following treatment with 2-picolinic acid (2-PA) in *Arabidopsis thaliana* seedlings and wheat (*Triticum aestivum*) leaf segments. Headspace ethylene concentration after 48 h (ppb) in sealed sample vessels and plant fresh weight (FW) at harvest are shown in panels **A** (*A. thaliana*) and **C** (wheat). Ethylene production normalized to FW is shown in panels **B** (*A. thaliana*) and **D** (wheat). Measurements were performed after 48 h of treatment and incubation. Data are presented as means ± SD. Statistical significance relative to untreated controls is indicated by asterisks in the colour of the data series (Welch's ANOVA with Dunnett's test, $p < 0.05$); n = 3–4 independent biological replicates.

2-Aminoisobutyric acid (AIB)

AIB, a structural analogue of ACC, was tested as a competitive inhibitor of ACO [33, 34, 35, 36] with the aim of identifying inhibitory effects that are not confounded by strong growth suppression or pleiotropic toxicity.

In Arabidopsis, AIB induced a moderate, concentration-dependent reduction of ethylene production detected consistently by both methods (Additional file 5). Production was already 21–23% lower than in controls at 10 µM, and the reduction reached at ≥ 50 µM increased gradually with dose, reaching 45–52% reduction at 1 000 µM (from 1.31 to 0.63 pmol·mg^{-1}·48h^{-1} by PAS; from 2.61 to 1.44 pmol·mg^{-1}·48h^{-1} by GC–FID). After normalization to FW the inhibitory trend remained stable. FW itself varied non-monotonically across the series (from 71 to 94 mg at 50 µM, returning to 75 mg at 1 000 µM) without a dose-dependent decline, so the reduction in ethylene output cannot be attributed to growth suppression.

Phytohormonal profiling revealed a progressive increase of ACC with increasing AIB concentration (from 368 to 2108 pmol·g^{-1}, a 5.7-fold rise), consistent with competitive inhibition of ACC utilization. Most other hormone classes declined with increasing AIB, the exception being abscisic acid (ABA) (Additional file 2).

In wheat, AIB was also inhibitory (Additional files 3 and 5). 100–1 000 µM reduced ethylene production by 17–27%, while ≥ 5 000 µM produced a measurable reduction in normalized emission (1.8- to 2.2-fold at 5 000 µM, rising to 2.5- to 3.3-fold at 10 000 µM). FW gained during incubation rose slightly up to 1 000 µM (from 14.6 to 18.0 mg) and fell at higher doses (from 12.4 mg at 10 000 µM), so inhibition at the top dose is partly concurrent with reduced growth. ACC levels increased with AIB concentration (from 1526 to ~ 3250–3460 pmol·g^{-1}), consistent with interference at the level of ACC metabolism rather than downstream perception, and off-target hormonal disturbances were less pronounced than in Arabidopsis.

Differential performance of ethylene biosynthesis inhibitors

Comparison of ACC synthase inhibitors and methodological implications

Among inhibitors of ACC synthase (ACS), AVG was clearly the most potent and specific compound in both *A. thaliana* and wheat. This observation is fully consistent with the irreversible inhibition of ACS through interaction with its pyridoxal-phosphate cofactor [28, 29] and with the long-standing agricultural use of AVG to suppress ethylene-dependent processes [26, 27]. Importantly, AVG strongly suppressed ethylene production without significantly affecting FW, making normalization particularly robust and confirming its suitability as a reference inhibitor in whole-plant assays.

Direct comparison of AOA and AVG responses highlights important differences in potency, specificity, and interpretability. While AVG inhibits ethylene biosynthesis in a dose-dependent manner with minimal collateral effects on growth or other hormones, the effect of AOA was weak and the difference between minimal effective and toxic dose was only one order of magnitude and even stimulatory in Arabidopsis, when recalculated per gram of FW. It induced also strong growth suppression from 500 µM and altered other hormones at all doses.”. These characteristics limit the use of AOA as a specific inhibitor of

ethylene biosynthesis, particularly in intact Arabidopsis seedlings. From a methodological perspective, AOA clearly demonstrates the importance of (i) delayed treatment application, (ii) normalization to biomass, and (iii) parallel hormone or other relevant compounds profiling to distinguish inhibition of ethylene biosynthesis from indirect effects caused by metabolic disruption or toxicity. These findings align with earlier reports of AOA and related aminooxy compounds efficacy in specific tissues such as cut flowers or fruits [36, 37] or specific cases such as mitigating effects of ethylene inducing treatments on fruits [31], while highlighting its limited suitability for whole-seedling assays due to pleiotropic toxicity.

Performance of ACO inhibitors

2-PA has been identified as an inhibitor of ACO on the basis of structural and enzymological evidence [18]. In the present whole-plant assays, it also inhibited growth at higher concentrations. Ethylene output per vial did not change, whereas FW-normalized production was slightly reduced at low concentrations and increased at growth-inhibiting ones.Phytohormonal profiling showed accumulation of ACC and strong activation of stress hormone pathways. In intact seedlings, the ethylene response to 2-PA therefore reflects both its effect on ACC conversion and its effect on growth, so FW normalization and concentrations below the growth-inhibiting threshold are important, when 2-PA is used in whole-plant assays. We would also point out that 6-indazolyl derivatives of 2-PA have been proposed as herbicides and shown to be effective. These compounds also promote ethylene release in Arabidopsis and unlike 2-PA itself, increase ABA production [32].

Compared with AVG, AIB represents an intermediate inhibitory phenotype. Its inhibitory efficacy is lower than that of AVG and is achieved without strong growth suppression or broad hormonal perturbations. These properties make AIB a useful supporting inhibitor for ethylene biosynthesis studies, especially when combined with normalization to biomass and phytohormonal controls. AIB required high concentrations, consistent with previous studies reporting competitive inhibition of ACO [33, 36] and delaying fruit ripening [38], but with comparatively fewer off-target hormonal effects compared to all tested ethylene production suppressors except AVG.

Ethylene precursors or donors

1-aminocyclopropane-1-carboxylic acid (ACC)

ACC, the immediate biosynthetic precursor of ethylene [39, 40, 41], was used as a positive control for ethylene induction and to evaluate the responsiveness and dynamic range of the parallel GC–FID/PAS measurement workflow across both plant systems.

In Arabidopsis seedlings, ACC treatment resulted in a strong, dose-dependent stimulation of ethylene production, as consistently detected by both GC–FID and PAS (Fig. 3; Additional file 2). Even low ACC concentrations (1 µM) caused a substantial increase in ethylene emission relative to untreated controls, and higher concentrations led to dramatic induction. At concentrations ≥ 10 µM ACC, ethylene production increased by more than an order of magnitude compared with controls. At the highest

concentrations tested, ethylene levels increased by two orders of magnitude (to 152.29 pmol·mg^{-1}·48h^{-1} by PAS, 258.27 pmol·mg^{-1}·48h^{-1} by GC) at 100 µM ACC relative to the untreated control (0.55 pmol·mg^{-1}·48h^{-1} by PAS, 3.01 pmol·mg^{-1}·48h^{-1} by GC). These levels exceeded the linear range of PAS operated in fine mode, necessitating reliance on coarse mode or GC–FID data for accurate quantification. Despite the pronounced ethylene production, plant FW remained relatively stable across the ACC concentration range. Regardless of normalization to FW, the stimulation of ethylene production remained robust, thus reflecting conversion of the supplied ACC to ethylene.

Phytohormonal analysis showed a marked accumulation of ACC in treated seedlings, proportional to the applied dose, while changes in other hormone classes were limited. This supports the interpretation that ACC acts predominantly as a direct input into ethylene biosynthesis and/or as a regulator with minimal (yet existing, as described by Van de poel *et al.* and Vanderstraeten *et al.* [42, 43]) pleiotropic effects under given conditions.

In wheat leaf segments, ACC also induced ethylene production in a clear concentration-dependent manner, though absolute ethylene levels were lower than in Arabidopsis (Fig. 3). Low ACC concentrations (1–5 µM) already stimulated ethylene production above background, and higher concentrations resulted in several-fold increases relative to controls, with a maximum increase of approximately one order of magnitude at 100 µM (from 0.60 to 8.09 pmol·mg^{-1}·48h^{-1} by PAS; from 0.69 to 9.07 pmol·mg^{-1}·48h^{-1} by GC–FID). FW was only weakly affected by ACC, and normalized ethylene production closely matched raw emission trends. ACC accumulation increased proportionally to treatment dose with limited changes in other phytohormones and ethylene itself, consistent with substrate uptake and effective conversion capacity of the ethylene biosynthetic machinery. Tissue ACC contents at the highest ACC concentrations should be interpreted with caution: besides ACC taken up into the cells, which in Arabidopsis roots is mediated by the LHT1 (LYSINE HISTIDINE TRANSPORTER1) transporter [44], part of the measured ACC may derive from treatment solution adhering to the plant surface or retained in the apoplast, as described for other compounds applied to roots [45].

Dose–response stimulation of ethylene production following application of 1-aminocyclopropane-1-carboxylic acid (ACC) in *Arabidopsis thaliana* seedlings and wheat (*Triticum aestivum*) leaf segments. Headspace ethylene concentration after 48 h (ppb) in sealed sample vessels and plant fresh weight (FW) at harvest are shown in panels **A** (*A. thaliana*) and **C** (wheat). Ethylene production normalized to FW is shown in panels **B** (*A. thaliana*) and **D** (wheat). Measurements were performed after 48 h of treatment and incubation. Data are presented as means ± SD. Statistical significance relative to untreated controls is indicated by asterisks in the colour of the data series (Welch's ANOVA with Dunnett's test, $p < 0.05$); n = 3–4 independent biological replicates.

Ethephon (ETH)

ETH (ethephon; 2-chloroethylphosphonic acid), a chemical ethylene-releasing compound [46, 47], reviewed by Kowsalya *et al.* [48], was used as a direct ethylene donor to distinguish effects of

endogenous ethylene biosynthesis from exogenously released ethylene and to further test the performance of the ethylene detection workflow.

In Arabidopsis seedlings, ETH caused strong increase in ethylene accumulation (Additional file 2 and 6). Even low ETH concentrations resulted in substantial ethylene release into the vial headspace. At moderate to high concentrations, ethylene levels frequently exceeded the linear detection range of PAS operated in fine mode, requiring coarse mode or GC-FID for accurate quantification. This behavior closely mirrored that observed for high ACC concentrations, confirming that GC–FID is more suited for quantifying strong ethylene outputs irrespective of their biological or chemical origin, as tripling the maximum dose would cause PAS saturation even in the coarse mode. FW of Arabidopsis seedlings was only moderately affected at lower ETH concentrations but declined noticeably at higher doses (≥ 500 µM; from 67.5 to 38.88 mg), indicating onset of phytotoxicity. After normalization to FW, ethylene production per unit biomass remained high (up to 429.81 pmol·mg^{-1}·48h^{-1} by PAS, 937.92 by GC compared to control: 0.65 pmol·mg^{-1}·48h^{-1} by PAS, 3.19 by GC), consistent with ETH acting primarily as a direct ethylene source rather than indirectly stimulating biosynthesis.

Phytohormonal analysis revealed no proportional increase in ACC levels in response to ETH treatment, clearly distinguishing its mode of action from ACC-induced ethylene production. Instead, changes in other hormone classes at higher doses (jasmonic acid (JA), salicylic acid (SA) and ABA increase at ≥ 500 µM) possibly reflected secondary stress responses triggered by elevated ethylene.

In wheat leaf segments, ETH also induced a robust increase in ethylene accumulation, with absolute ethylene levels higher than in Arabidopsis (Additional file 3 and 6). FW of wheat leaf tissue increased from 15.0 mg to 22.0 mg at 500 µM and 19.8 mg at 1 000 µM. As in Arabidopsis, normalization to FW confirmed that changed tissue mass contributed only minimally to observed changes in total ethylene accumulation (from 0.52 to 248.28 pmol·mg^{-1}·48h^{-1} by PAS; from 0.72 to 293.93 pmol·mg^{-1}·48h^{-1} by GC–FID at 1 000 µM).

ACC content in wheat decreased with increasing ETH concentration (by 50% at 1 000 µM), consistent with ethylene release independent of the endogenous biosynthetic pathway [48]. SA, ABA and JA also decreased (by 32–60% at 1 000 µM), whereas free IAA and its metabolites changed only little (Additional file 3).

Comparison of ACC and ETH, methodological implications

Compounds acting as ethylene precursors or donors behaved predictably within the unified workflow. ACC induced robust, dose-dependent ethylene production in both species, consistent with its central role as the direct ethylene precursor [39, 40, 41]. The strong correlation between ACC levels and ethylene production observed in phytohormonal analyses of other treatments further validates the biochemical coherence of the dataset. Although ACC can also act as an ethylene-independent growth regulator [42, 43], such effects could not be separated here from the resulting ethylene modulations. ACC treatment represents a suitable positive control for validating ethylene measurement approaches. The strong and

predictable stimulation of ethylene biosynthesis across two plant species demonstrates that the parallel GC–FID/PAS workflow is sensitive, quantitative, and capable of resolving large dynamic changes in ethylene production. In addition, the ACC data clearly illustrate the complementary strengths of both analytical methods: PAS provides rapid and sensitive detection for low-to-moderate ethylene concentrations, while GC–FID is required for accurate quantification of high ethylene outputs induced by large doses of strong precursors or donors.

ETH, as expected, released ethylene independently of endogenous biosynthesis, producing high ethylene outputs even in the absence of ACC accumulation [46, 47]. However, substantial ethylene release from treated medium alone (data not shown, self decomposition, esp. in alkalic enviroments desribed by Yang [47] emphasizes the necessity of rigorous medium-only controls, particularly in Murashige-Skoog-based media.

Comparison of ACC and ETH responses clearly differentiates endogenous ethylene biosynthesis from exogenous ethylene release. While both treatments result in high ethylene levels, only ACC increases ACC content and follows enzymatic dose–response characteristics, whereas ETH bypasses metabolic control and leads to immediate ethylene liberation. From a methodological standpoint, ETH provides a stringent test of analytical capacity under conditions of high ethylene load. The excellent agreement between GC–FID and PAS at low concentrations, combined with predictable PAS saturation in fine mode and approaching the saturation range of coarse mode at high ethylene levels, further validates the complementary use of both methods within the same experimental workflow.

Cytokinin-like compounds

Thidiazuron (TDZ)

TDZ is a highly active synthetic cytokinin that stimulates ethylene production in plant tissues, which often leads to enhanced leaf abscission and defoliation, particularly in cotton [49, 50, 51]. It was included as a representative of hormonally indirect ethylene modulators.

In Arabidopsis seedlings, TDZ induced a clear and concentration-dependent stimulation of ethylene production (Additional file 2 and 7). Detectable ethylene induction was already observed at low TDZ concentrations (0.5–1 µM), with further increases at higher doses. Unlike ACC or ETH, TDZ-induced ethylene production showed a relatively shallow dose–response curve, suggesting indirect activation mechanisms rather than direct metabolic flux. FW of Arabidopsis seedlings increased gradually with increasing TDZ concentration, particularly at higher doses (from 66.93 to 76.0 mg FW), indicating cytokinin-associated growth stimulation. After normalization to FW, TDZ remained a moderate but reproducible inducer of ethylene production (from 1.08 to 3.18 $pmol \cdot mg^{-1} \cdot 48h^{-1}$ by PAS; from 3.30 to 9.15 $pmol \cdot mg^{-1} \cdot 48h^{-1}$ by GC–FID at 50 µM), showing that the stimulatory effect could not be attributed solely to biomass changes.

Phytohormonal analysis revealed strong alterations in some cytokinin profiles including pronounced decreases in active cytokinin forms and their ribosides, accompanied by secondary changes in IAA and stress-related hormones (↑SA, ↓JA). ACC levels showed no proportional increase corresponding to ethylene induction, indicating that TDZ stimulates ethylene production primarily through regulatory signaling pathways rather than by directly enhancing ACC pool size.

In wheat leaf segments, TDZ also stimulated ethylene production, but the response was weaker and less concentration-sensitive than in Arabidopsis (Additional file 3 and 7). Low TDZ concentrations resulted in minimal ethylene induction, whereas higher doses (≥ 5μM) produced a higher plateau response in ethylene emission (from 0.73 to 1.74 pmol·mg^{-1}·48h^{-1} by PAS; from 0.62 to 1.64 pmol·mg^{-1}·48h^{-1} by GC–FID at 5 μM). FW of wheat tissue showed only non-significant increases, suggesting reduced sensitivity of wheat leaf segments to cytokinin-mediated growth effects compared with intact Arabidopsis seedlings.

Hormonal profiling in wheat revealed TDZ-driven increases in less active cytokinin [*c*Z (*cis*-zeatin), *c*ZR (*cis*-zeatin riboside), iPR (isopentenyladenosine)] levels with secondary hormonal perturbations (ABA decreased by 71–80% at all doses, Additional file 3), consistent with a conserved but attenuated cytokinin-ethylene interaction in monocot leaf tissue.

Comparison with ethylene precursors and inhibitors

TDZ, although not a direct ethylene biosynthesis regulator, consistently induced moderate ethylene production, accompanied by increases in *c*Z, *c*ZR and iPR in wheat and decreases in *t*Z, iP, *t*ZR and iPR in Arabidopsis. The lack of correlated ACC increases in cut wheat leaves confirms that TDZ can stimulate ethylene indirectly via hormonal signaling networks, consistent with its role in cytokinin–ethylene crosstalk during leaf abscission and defoliation [49, 50, 51]. In contrast to this, in the whole Arabidopsis seedling system, ACC levels correlate with treatment dose strongly (R = 0.87). The tendency towards increase in FW is also consistent with earlier reports [52].

In contrast to ACC and ETH, TDZ induces ethylene production indirectly through hormonal signaling [50, 51, 53] and delayed ethylene stimulation. Compared with cytotoxic inhibitors such as 2-PA or high-dose AOA, TDZ effects are less pleiotropic, yet clearly distinguishable from biosynthetic activation. From a methodological perspective, TDZ provides a valuable example of signal-mediated ethylene induction, highlighting the necessity of integrating phytohormonal profiling with ethylene measurements to avoid oversimplified interpretations.

Signalling modulators

Silver thiosulfate (STS)

STS acts as a potent anti-ethylene agent by blocking ethylene receptors, inhibiting its ability to accelerate senescence, abscission, and ripening in plants [54, 55]. It was included to assess how disruption of ethylene signalling influences measured ethylene production and to distinguish biosynthesis-related effects from perception-dependent feedback regulation.

In Arabidopsis seedlings, STS application resulted in significant and reproducible changes in ethylene production (Additional file 2 and 8). Contrary to biosynthesis inhibitors, STS did not strongly suppress ethylene emission. Instead, ethylene production was elevated even at lowest doses. The increase in ACC and ethylene production following STS treatment is consistent with disruption of ethylene-dependent feedback regulation of the biosynthetic pathway (described by Chang et al. [56]), although the underlying molecular mechanisms were not directly examined in this study. At higher STS concentrations, Arabidopsis FW decreased significantly (from 79.85 to 49.40 mg), consistent with Ag^{+} toxicity [57] with visible growth inhibition. After normalization to FW, ethylene production per unit biomass dose-dependently increased (from 1.95 to 48.32 pmol·mg^{-1}·$48h^{-1}$ by PAS; from 3.24 to 57.06 pmol·mg^{-1}·$48h^{-1}$ by GC–FID), confirming that the observed effects were not driven by biomass changes.

Phytohormonal profiling also revealed increase in ACC levels (from 680 to 32 245 pmol·g^{-1}), further supporting the notion that STS directly targets ethylene perception, while the observed accumulation of ACC and increased ethylene production indicate substantial secondary effects on ethylene biosynthetic regulation. In parallel, pronounced alterations in multiple stress hormone pathways were observed, including strong concentration-dependent increases in SA and JA hormones (Additional file 2).

In wheat leaf segments, STS exhibited a weaker, but comparable effect on ethylene production (Additional file 3 and 8). At low concentrations, ethylene emission per unit FW remained largely unchanged compared with controls, while higher concentrations (≥ 500 µM) resulted in ca sixfold increase (from 0.82 to 4.70 pmol·mg^{-1}·$48h^{-1}$ by PAS; from 0.71 to 4.52 pmol·mg^{-1}·$48h^{-1}$ by GC–FID). Wheat FW remained unchanged.

ACC levels increased steadily with dose (from 662 up to 7222 pmol·g^{-1}) across STS treatments, suggesting a feedback activation of ethylene biosynthesis in excised wheat leaf tissue. Hormonal profiling in wheat leaves revealed modest secondary hormonal perturbations, specifically fo SA and JA.

Mebendazole (MEB)

MEB is a benzimidazole compound that activates ethylene signaling by inhibiting the CTR1 (CONSTITUTIVE TRIPLE RESPONSE1) kinase. This interaction causes MEB to mimic the effects of ethylene, leading to distinct changes in root system architecture, such as increased lateral root angles [17]. It was included as a signaling modulator acting downstream of ethylene perception.

In Arabidopsis seedlings, MEB treatment resulted in a moderate, concentration-dependent increase in ethylene production (Additional file 2 and 9). Ethylene stimulation became evident at concentrations ≥

0.5 µM and increased gradually with dose. FW of seedlings was not affected. After normalization to FW, ethylene production remained elevated reaching ~ 1.6-1.7-fold induction compared with control (from 1.46 to 2.60 pmol·mg^{-1}·48h^{-1} by PAS; from 3.08 to 5.04 pmol·mg^{-1}·48h^{-1} by GC–FID at 50 µM).

Phytohormonal analysis revealed only a small increase in ACC concentration, suggesting that MEB-induced ethylene production does not primarily result from enhanced biosynthetic flux. Instead, limited changes in hormone profiles support the interpretation that MEB influences ethylene output indirectly through signalling or structural regulation rather than direct enzymatic control.

In contrast to Arabidopsis, MEB did not change ethylene production in wheat (0.57–0.64 vs 0.64 pmol·mg^{-1}; Additional file 3 and 9). FW of wheat tissue showed limited sensitivity to MEB, and absolute ethylene levels remained stable across treatments. ACC did not increase.

The doses of MEB used were lower compared to other treatments used, as its poor solubility made use of higher doses impossible.

Context within ethylene modulation mechanisms

Compounds interfering with ethylene perception or signaling exhibited distinct ethylene production patterns. STS, an inhibitor of ethylene perception via silver–copper substitution in ETHYLENE RESPONSE1 (ETR1) [54, 55], did not suppress ethylene biosynthesis. Instead, increases in ethylene production at moderate concentrations were observed, consistent with disruption of negative feedback regulation of ethylene biosynthesis following receptor inhibition [56]. This behavior reinforces the need to distinguish clearly between ethylene production and ethylene perception when interpreting phenotypic outcomes. The STS response pattern clearly differs from that of direct biosynthesis inhibitors such as AVG, or AIB. While those compounds reduce ethylene production through interference with enzymatic steps of the biosynthetic pathway, STS does not suppress ethylene formation but rather may allow its production to increase by releasing feedback inhibition, as demonstrated here. These results reinforce the importance of distinguishing ethylene biosynthesis, perception, and signaling when interpreting ethylene-related phenotypes. Measurement of ethylene emission alone is insufficient to infer signaling activity unless combined with signaling modulators such as STS.

MEB, recently identified as a CTR1 kinase inhibitor [17], induced modest ethylene increases in Arabidopsis but not in wheat at comparable concentrations. The absence of ACC accumulation suggests that MEB affects ethylene output primarily through signaling-level modulation rather than biosynthetic activation, complementing recent molecular studies and highlighting species-dependent sensitivity. In contrast to canonical biosynthesis inhibitors (AVG, AOA, AIB) or direct donors (ACC, ETH), MEB represents a signaling-level modulator of ethylene production. Its effects are moderate and species-dependent, and associated regulatory pathways rather than direct control of ethylene biosynthetic enzymes [17].

LC-MS/MS (liquid chromatography-tandem mass spectrometry) phytohormonal analysis and correlations

Pearson correlations between ACC and phytohormone contents, ethylene production and FW (Fig. 4, 5), and with the applied dose (Fig. 6, 7), were calculated. To complement ethylene measurements, we performed a LC–MS/MS based phytohormonal profiling of the same biological samples used for gas analysis, enabling direct integration of ethylene production with broader hormone homeostasis. Across both Arabidopsis seedlings and wheat leaf segments, multiple phytohormone classes—including ACC, cytokinins, auxins and their conjugates, ABA, SA, and jasmonates - were quantified and subjected to correlation analysis with ethylene output, treatment concentration, and FW (Additional file 10, Additional file 11).

Across Arabidopsis datasets, ethylene production showed an exceptionally strong positive correlation with ACC levels, typically approaching near linear dependence when excluding treatments directly supplying ACC or releasing ethylene (ETH). ACC showed strong positive correlations with ethylene measured by both PAS and GC–FID ($r \approx 0.78$ when ACC or ETH treatments were not included; Additional file 10). This relationship remained highly consistent across independent treatment series and analytical platforms, confirming that ACC availability represents important limiting factor for ethylene biosynthesis under the applied experimental conditions. In contrast, wheat leaf segments displayed weaker and more variable ACC–ethylene correlations. This reduced coupling likely reflects additional sources of biological variability inherent to excised tissue systems, including wound induced responses and altered metabolic regulation, rather than differences in analytical performance.

All quantified cytokinin metabolites (*t*Z, *c*Z, iP, and their ribosides – except *c*ZR) exhibited strong positive correlations among themselves in both plant systems. However, these cytokinin pools were largely uncorrelated with ethylene production or ACC levels, indicating that cytokinin homeostasis operates predominantly independently of ethylene biosynthesis in this experimental context. Notably, cytokinin active compound TDZ induced changes of cytokinin metabolites. In wheat, TDZ increased *c*Z, *c*ZR and *i*PR about threefold, together with ethylene (2.4–2.7-fold) and ACC (1.6–2.0-fold); in Arabidopsis it decreased *t*Z, iP, *t*ZR and iPR. This further supports the conclusion that cytokinin-driven responses are largely orthogonal to ethylene output.

Free IAA showed only weak and inconsistent relationships with ethylene production across treatments. In contrast, auxin conjugates and oxIAA changed strongly under some growth-inhibiting treatments, in either direction depending on compound and species (e.g., high-dose AOA or 2-PA). These patterns indicate that auxin metabolism in this system primarily reflects inactivation and turnover processes linked to stress or impaired growth, rather than direct regulatory coupling to ethylene biosynthesis.

Jasmonates (JA and JA-Ile) showed positive correlations with ethylene predominantly under stress-inducing treatments, such as MEB, suggesting coordinated activation of stress-responsive pathways. In contrast, ABA and, partly, SA were more strongly associated with growth inhibition and biomass

reduction than with ethylene production per se. Importantly, ABA frequently exhibited negative correlations with ethylene output under inhibitory conditions, reflecting opposing physiological trends between stress-induced growth suppression and active ethylene biosynthesis.

Importantly, when ACC and ETH treatments were excluded from the analysis, correlations between ethylene and other hormone classes have intensified substantially. This demonstrates that most cross-hormone correlations are driven by treatment structure rather than intrinsic co-regulation, reinforcing the importance of pathway-specific interpretation.

Pearson coefficients were calculated from the 54 treatment–dose means; ethylene was measured by PAS (ETD-300) and GC–FID, see Additional file 10.

Species-specific aspects of hormonal integration

While general trends were conserved, several differences between Arabidopsis and wheat were apparent. Arabidopsis seedlings were generally more sensitive to treatments than wheat leaf segments, and toxicity thresholds differed markedly between species. In wheat, correlations between ethylene and other hormone classes were overall weaker, whereas stress-associated markers such as jasmonates and auxin catabolites showed stronger responses, likely reflecting tissue damage and wound signalling inherent to the leaf segment assay. Similarly, ABA correlations were less consistent in wheat, and cytokinin–ethylene independence was even more pronounced. These differences highlight that species and experimental system strongly influence apparent hormone networks, emphasizing the importance of consistent experimental conditions for comparative analyses.

Cytokinin metabolites again formed a strongly correlated internal module, but showed even less association with ethylene. This supports the conclusion that cytokinin–ethylene crosstalk is attenuated in wheat leaf segments under the applied conditions. Auxin-related metabolites displayed limited correlations with ethylene, except under treatments causing marked tissue damage (e.g., 2-PA at high concentrations), where auxin conjugates and oxIAA increased in parallel with stress-associated hormones. As in Arabidopsis, these correlations reflect secondary metabolic responses rather than regulatory control of ethylene biosynthesis. JA and JA-Ile showed sporadic positive associations with ethylene, particularly under treatments that stimulated stress responses without directly supplying ACC. However, these relationships were weaker and less consistent than in Arabidopsis. ABA correlations were predominantly negative or weak, suggesting that ABA accumulation largely accompanies growth reduction rather than ethylene modulation per se. FW showed strong negative correlations with several treatments (notably 2-PA and STS), confirming that growth suppression is a major confounding factor influencing apparent ethylene emission when data are not normalized. When ACC and ETH treatments were excluded, correlations between ethylene and other hormones were generally weak, underscoring that ethylene production in wheat is less tightly integrated into global hormonal networks than in Arabidopsis. These findings further emphasize the importance of combining ethylene measurements with broader hormonal profiling to avoid oversimplified interpretations.

Pearson coefficients were calculated from the 54 treatment–dose means; ethylene was measured by PAS (ETD-300) and GC–FID, see Additional file 11.

Integrated interpretation

FW is a critical determinant of apparent hormonal relationships, because plant FW exhibited strong negative correlations with ethylene under treatments causing growth inhibition or toxicity (e.g. 2-PA or STS). This effect demonstrates that apparent hormonal interactions can be dominated by biomass-related artefacts when normalization is not applied. Normalization of ethylene and hormone levels to FW therefore proved essential for correct biological interpretation and for avoiding false conclusions about inhibitory or stimulatory effects. Across both plant systems, correlation analysis confirms that ACC availability is an important determinant of ethylene production, while most other apparent hormone–ethylene relationships arise indirectly from treatment-specific stress or growth effects. Cytokinin-mediated ethylene induction (e.g., under TDZ treatment) operates predominantly at the signaling level. Stress hormones and auxin catabolites closely track tissue damage, biomass reduction, and metabolic impairment, particularly under non-specific inhibitors such as 2-PA. These findings emphasize that correlation-based interpretation without normalization and pathway context would lead to erroneous conclusions regarding ethylene regulation. Overall, LC-MS/MS phytohormone profiling of the same samples helped to distinguish effects on ethylene biosynthesis from growth-related or other effects.

Correlation analysis between applied treatment concentrations and endogenous phytohormone levels in Arabidopsis. Pearson correlation coefficients illustrate dose-dependent hormonal responses across all treatments, calculated within each compound series (six dose levels including the untreated control).

Correlation analysis between applied treatment concentrations and endogenous phytohormone levels in wheat (Triticum aestivum) leaf segments. Pearson correlation coefficients illustrate dose-dependent hormonal responses across all treatments, calculated within each compound series (six dose levels including the untreated control). <LOD – below limit of detection (thus not included in correlation).

Limitations and broader implications

Several limitations should be acknowledged. Formal determination of limit of detection and limit of quantification values for both analytical platforms was beyond the scope of this study, although practical detection limits were empirically established. Solubility constrained the concentration range for MEB, and the wheat leaf assay, while highly reproducible, does not fully replicate whole-plant physiology. Finally, seedling-based systems cannot capture all regulatory layers operative in mature plants.

Despite these limitations, our results demonstrate that consistency of experimental design - particularly delayed treatment application and FW normalization - can substantially improve the reliability and comparability of ethylene measurements across studies. The parallel GC–FID/PAS workflow provides a flexible and robust platform for systematic evaluation of ethylene-modulating compounds and can be

readily integrated with LC–MS/MS-based phytohormone profiling. Together, these approaches offer a powerful foundation for future studies addressing ethylene biosynthesis, signaling, and hormonal crosstalk in diverse plant systems.

Conclusion

Ethylene research has benefited from major advances in analytical instrumentation, including highly sensitive GC-based methods and laser-driven photoacoustic spectroscopy. Protocols differ between studies, which redues comparability

Here, we present a unified workflow that combines GC-FID and PAS measurements with consistent experimental design, FW normalization, and compatibility with downstream LC-MS/MS phytohormonal profiling. Direct comparison of both methods using identical biological samples demonstrated strong agreement across treatments and species. PAS provided rapid and sensitive quantification of low-to-moderate ethylene production, whereas GC-FID offered better linearity and robustness at high ethylene concentrations.

Application of the workflow to nine ethylene-modulating compounds in Arabidopsis and wheat revealed pronounced species-specific responses and highlighted the importance of biomass normalization for correct interpretation of treatment effects. Among the tested inhibitors, AVG displayed the highest specificity and efficacy, whereas responses to AOA and 2-PA were strongly influenced by growth inhibition and broader physiological effects. Correlation analyses further confirmed that ACC availability is key determinant of ethylene production, while many apparent associations with other hormones reflect indirect stress- or growth-related responses.

Overall, the proposed GC-FID/PAS workflow provides a robust and reproducible platform for ethylene quantification and interpretation. Its integration with phytohormonal profiling offers a practical framework for future studies of ethylene biosynthesis, signaling, and hormone interactions across diverse plant systems.

In summary, while many powerful tools for ethylene detection already exist, the workflow presented in this study provides a conceptual and practical bridge between analytical precision, biological relevance, and hormonal systems integration. It offers a foundation for future studies seeking to place ethylene production into a broader physiological framework rather than treating it as an isolated output variable.

Declarations

Acknowledgements

We would like to offer our thanks to Hana Vylíčilová (Department of Chemical Biology, Faculty of Science, Palacký University Olomouc, Šlechtitelů 27, 779 00 Olomouc, Czech Republic) for kindly providing wheat seedlings.

Authors' contributions

JS, MS and MK proposed the basic concept. JS, MK and JM proposed and optimised the instrumental methodology. JS and MK proposed the workflow. JS created parts of sampling system, optimized the workflow, cultivated plants, applied treatments, conducted ethylene measurements and processed samples. KC and MK conducted measurements of other phytohormones. JS evaluated data, reviewed literature, created figures and tables and wrote the manuscript draft. JS and MS modified the manuscript draft into pre final form. JS and MK finalized the manuscript, KC provided insights to the text when necessary. JS and MK edited and corrected the final manuscript. All authors proofread and approved the manuscript. MS supervised the work as a whole and acquired funding. MK supervised the experimental part and provided consultation regarding instrument use.

Funding

The presented work was supported by Internal Grant Agency of Palacký University IGA_PrF_2026_014.

The work was supported from European Regional Development Fund-Project " SMART Plant Biotechnology for Sustainable Agriculture " (No. CZ.02.01.01/00/23_020/0008497) co-funded by the European Union.

KC acknowledges support of ERC Synergy project “Unravelling Spatio-temporal Auxin Intracellular Redistribution for Morphogenesis” (STARMORPH, reg. no. 101166880).

Competing interests

The authors declare that they have no competing interests.

Availability of data and materials

All evaluated data generated or analysed during this study are included in this published article and its supplementary information files. Raw data from instruments are available the Zenodo repository, https://doi.org/10.5281/zenodo.23312413

Consent to participate and ethics approval

Not applicable

Consent for publication

Not applicable

References

1. Li W, Li Q, Lyu M, Wang Z, Song Z, Zhong S, et al. Lack of ethylene does not affect reproductive success and synergid cell death in Arabidopsis. Mol Plant. 2022;15(2):354–62. 10.1016/j.molp.

.2021.11.001 PubMed PMID: 34740849.

2. Heydlauff J, Serbes IE, Vo D, Mao Y, Gieseking S, Nakel T, et al. Dual and opposing roles of EIN3 reveal a generation conflict during seed growth. Mol Plant. 2022;15(2):363–71. 10.1016/j.molp. .2021.11.015 PubMed PMID: 34848348.
3. Kathirvelan J, Vijayaraghavan R. Review on sensitive and selective ethylene detection methods for fruit ripening application. Sens Rev. 2020;40(4):421–35. 10.1108/SR-10-2019-0251.
4. Chen X, Wreyford R, Nasiri N. Recent Advances in Ethylene Gas Detection. Materials. 2022;15(17):5813. 10.3390/ma15175813.
5. Burg SP, Burg EA. Role of Ethylene in Fruit Ripening. Plant Physiol. 1962;37(2):179–89. 10.1104/pp. .37.2.179 PubMed PMID: 16655629; PubMed Central PMCID: PMC549760.
6. Kaur K, Singh R, Kaur G. A Comparative Study of Ethylene Detection Methods in Fruit Supply Chains: a Review. Food Anal Methods. 2024;17(1):14–32. 10.1007/s12161-023-02545-x.
7. Woltering EJ, Harren F, Boerrigter HAM. Use of a Laser-Driven Photoacoustic Detection System for Measurement of Ethylene Production in Cymbidium Flowers. Plant Physiol. 1988;88(2):506–10. 10.1104/pp.88.2.506.
8. Cristescu SM, Mandon J, Arslanov D, De Pessemier J, Hermans C, Harren FJM. Current methods for detecting ethylene in plants. Ann Bot. 2013;111(3):347–60. 10.1093/aob/mcs259.
9. an de Poel B. Plant Ethylene Detection Using Laser-Based Photo-Acoustic Spectroscopy. In: Binder BM, Eric Schaller G, editors. Ethylene Signaling: Methods and Protocols [Internet]. New York, NY: Springer; 2017 [cited 2026 Jun 25]. pp. 11–26. Available from: https://doi.org/10.1007/978-1-4939-6854-1_2 doi:10.1007/978-1-4939-6854-1_2.
10. Gwanpua SG, Jabbar A, Tongonya J, Nicholson S, East AR. Measuring ethylene in postharvest biology research using the laser-based ETD-300 ethylene detector. Plant Methods. 2018;14(1):105. 10.1186/s13007-018-0372-x.
11. Saliu F, Biale G, Raguso C, La Nasa J, Degano I, Seveso D, et al. Detection of plastic particles in marine sponges by a combined infrared micro-spectroscopy and pyrolysis-gas chromatography-mass spectrometry approach. Sci Total Environ. 2022;819:152965. 10.1016/j.scitotenv.2022.152965.
12. Desbrosses G, Cartieaux F, Rodrigues O, Boutin F, Vicet A, Touraine B, et al. Physical and Biological Measurements of Ethylene Emission Pinpoint the Importance of EIN4, EIN3 and EIL1 in the Regulation of Ethylene Biosynthesis in Arabidopsis Thaliana. J Plant Growth Regul. 2026;45(3):2422–35. 10.1007/s00344-025-12020-y.
13. Urdin-Bravo M, Sanchez-Garcia A, Rodriguez-Concepcion M, Martinez-Garcia JF. Effect of Higher Ethylene Levels Emitted by Shade-Avoider Plants on Neighboring Seedlings. Plants. 2024;13(22):3212. 10.3390/plants13223212.
14. Mockevičiūtė R, Jurkonienė S, Šveikauskas V, Zareyan M, Jankovska-Bortkevič E, Jankauskienė J, et al. Probiotics, Proline and Calcium Induced Protective Responses of Triticum aestivum under Drought Stress. Plants. 2023;12(6):1301. 10.3390/plants12061301.

15. Yoon GM, Chen YC. Gas Chromatography-Based Ethylene Measurement of Arabidopsis Seedlings. In: Binder BM, Eric Schaller G, editors. Ethylene Signaling: Methods and Protocols [Internet]. New York, NY: Springer; 2017 [cited 2026 Jun 25]. pp. 3–10. Available from: https://doi.org/10.1007/978-1-4939-6854-1_1 doi:10.1007/978-1-4939-6854-1_1.
16. Van Der Depaepe T. Tools of the Ethylene Trade: A Chemical Kit to Influence Ethylene Responses in Plants and Its Use in Agriculture. Small Methods. 2020;4(8):1900267. 10.1002/smtd.201900267.
17. He W, Truong HA, Zhang L, Cao M, Arakawa N, Xiao Y, et al. Identification of mebendazole as an ethylene signaling activator reveals a role of ethylene signaling in the regulation of lateral root angles. Cell Rep. 2024;43(2). 10.1016/j.celrep.2024.113763 . PubMed PMID: 38358890.
18. Sun X, Li Y, He W, Ji C, Xia P, Wang Y, et al. Pyrazinamide and derivatives block ethylene biosynthesis by inhibiting ACC oxidase. Nat Commun. 2017;8(1):15758. 10.1038/ncomms15758.
19. Le Deunff E, Lecourt J. Non-specificity of ethylene inhibitors: 'double-edged' tools to find out new targets involved in the root morphogenetic programme. Plant Biol. 2016;18(3):353–61. 10.1111/plb.12405.
20. Karady M, Hladík P, Cermanová K, Jiroutová P, Antoniadi I, Casanova-Sáez R, et al. Profiling of 1-aminocyclopropane-1-carboxylic acid and selected phytohormones in Arabidopsis using liquid chromatography-tandem mass spectrometry. Plant Methods. 2024;20(1):41. 10.1186/s13007-024-01165-8.
21. Holub J, Hanuš J, Hanke DE, Strnad M. Biological activity of cytokinins derived from Ortho- and Meta-Hydroxybenzyladenine. Plant Growth Regul. 1998;26(2):109–15. 10.1023/A:1006192619432.
22. Cermanová K, Bublavá P, Darbandsari M, Fellner M, Novák O, Karady M. Metabolic network divergence: polyamine and ethylene biosynthesis dynamics in Arabidopsis thaliana and Solanum lycopersicum. Plant Stress. 2025;18:101124. 10.1016/j.stress.2025.101124.
23. Pereira L, Pujol M, Garcia-Mas J, Phillips MA. Non-invasive quantification of ethylene in attached fruit headspace at 1 p.p.b. by gas chromatography–mass spectrometry. Plant J. 2017;91(1):172–83. 10.1111/tpj.13545.
24. Hermans C, Porco S, Vandenbussche F, Gille S, De Pessemier J, et al. Dissecting the Role of CHITINASE-LIKE1 in Nitrate-Dependent Changes in Root Architecture. Plant Physiol. 2011;157(3):1313–26. 10.1104/pp.111.181461.
25. Vaseva II, Qudeimat E, Potuschak T, Du Y, Genschik P, Vandenbussche F et al. The plant hormone ethylene restricts Arabidopsis growth via the epidermis. Proceedings of the National Academy of Sciences. 2018;115(17):E4130–9. 10.1073/pnas.1717649115
26. Beltrano J, Ronco MG, Montaldi ER. Drought Stress Syndrome in Wheat Is Provoked by Ethylene Evolution Imbalance and Reversed by Rewatering, Aminoethoxyvinylglycine, or Sodium Benzoate. J Plant Growth Regul. 1999;18(2):59–64. 10.1007/PL00007049.
27. Tipu MMH, Sherif SM. Ethylene and its crosstalk with hormonal pathways in fruit ripening: mechanisms, modulation, and commercial exploitation. Front Plant Sci. 2024;15. 10.3389/fpls.2024.1475496.

28. Boller T, Herner RC, Kende H. Assay for and enzymatic formation of an ethylene precursor, 1-aminocyclopropane-1-carboxylic acid. Planta. 1979;145(3):293–303. 10.1007/BF00454455.
29. Capitani G, McCarthy D, Gut H, Grütter M. Apple 1-aminocyclopropane-1-carboxylate synthase in complex with the inhibitor L-aminoethoxyvinylglycine: Evidence for a ketimine intermediate. J Biol Chem. 2002;277(51):49735–42. 10.1074/jbc.M208427200.
30. Amrhein N, Wenker D. Novel inhibitors of ethylene production in higher plants. Plant Cell Physiol. 1979;20(8):1635–42. 10.1093/oxfordjournals.pcp.a075966.
31. Wang J, Bai P, Feng J, He Y, Wu Y, Yu J, et al. Exogenous ALA accelerates tomato fruits softening by promoting cell wall degradation in an ethylene-dependent manner. Sci Hort. 2025;342:114055. 10.1016/j.scienta.2025.114055.
32. Liu Q, Shi RC, Li HT, Wei W, Yuan X, Liu SZ, et al. Study on Design, Synthesis and Herbicidal Activity of Novel 6-Indazolyl-2-picolinic Acids. Molecules. 2024;29(2):332. 10.3390/molecules29020332.
33. Satoh S, Esashi Y. α-Aminoisobutyric acid: A probable competitive inhibitor of conversion of 1-aminocyclopropane-1-carboxylic acid to ethylene. Plant Cell Physiol. 1980;21(6):939–49. 10.1093/oxfordjournals.pcp.a076082.
34. Satoh S, Esashi Y. α-Aminoisabutyric acid, propyl gallate and cobalt ion and the mode of inhibition of ethylene production by cotyledonary segments of cocklebur seeds. Physiol Plant. 1983;57(4):521–6. 10.1111/j.1399-3054.1983.tb02779.x.
35. Serrano M, Romojaro F, Casas JL, Del Rio JA, Acosta M. Action and mechanism of α-aminoisobutyric acid as a retardant of cut carnation senescence. Sci Hort. 1990;44(1):127–34. 10.1016/0304-4238(90)90023-8.
36. Kosugi Y, Matsuoka A, Higashi A, Toyohara N, Satoh S. 2-Aminooxyisobutyric acid inhibits the in vitro activities of both 1-Aminocyclopropane-1-carboxylate (ACC) synthase and ACC oxidase in ethylene biosynthetic pathway and prolongs vase life of cut carnation flowers. J Plant Biol. 2014;57(4):218–24. 10.1007/s12374-014-0180-4.
37. Fujino DW, Reid MS, EFFECTS OF AMINOOXYACETIC SY, ACID ON POSTHARVEST CHARACTERISTICS OF CARNATION. Acta Hort. 1981;11359–64. 10.17660/actahortic.1981.113.8.
38. Rajeswari V, Jeyakumar P, Kalarani MK, Subramanian KS, Kavino M, Djanaguiraman M. Improvement in the shelf life of banana is associated with membrane destabilising enzyme activity. Plant Physiol Rep. 2023;28(1):142–51. 10.1007/s40502-023-00710-2.
39. Yu YB, Adams DO, Yang SF. 1-Aminocyclopropanecarboxylate synthase, a key enzyme in ethylene biosynthesis. Arch Biochem Biophys. 1979;198(1):280–6. 10.1016/0003-9861(79)90420-X.
40. Adams DO, Yang SF. Ethylene biosynthesis: Identification of 1-aminocyclopropane-1-carboxylic acid as an intermediate in the conversion of methionine to ethylene. Proceedings of the National Academy of Sciences. 1979;76(1):170–4. 10.1073/pnas.76.1.170
41. Ververidis P, John P. Complete recovery in vitro of ethylene-forming enzyme activity. Phytochemistry. 1991;30(3):725–7. 10.1016/0031-9422(91)85241-Q.

42. an de Poel B. 1-aminocyclopropane-1-carboxylic acid (ACC) in plants: more than just the precursor of ethylene! Front Plant Sci. 2014;5. 10.3389/fpls.2014.00640.
43. Vanderstraeten L, Depaepe T, Van Der Bertrand S. The Ethylene Precursor ACC Affects Early Vegetative Development Independently of Ethylene Signaling. Front Plant Sci. 2019;10. 10.3389/fpls.2019.01591.
44. Shin K, Lee S, Song WY, Lee RA, Lee I, Ha K, et al. Genetic Identification of ACC-RESISTANT2 Reveals Involvement of LYSINE HISTIDINE TRANSPORTER1 in the Uptake of 1-Aminocyclopropane-1-Carboxylic Acid in Arabidopsis thaliana. Plant Cell Physiol. 2015;56(3):572–82. 10.1093/pcp/pcu201.
45. Liu Y, Tao Z, Lu H, Li S, Hu C, Li Z. Electrochemical properties of roots determine antibiotic adsorption on roots. Front Plant Sci. 2023;14. 10.3389/fpls.2023.930632.
46. Cooke AR, Randall DI. 2-Haloethanephosphonic Acids as Ethylene Releasing Agents for the Induction of Flowering in Pineapples. Nature. 1968;218(5145):974–5. 10.1038/218974a0.
47. Yang SF. Ethylene Evolution From 2-Chloroethylphosphonic Acid. Plant Physiol. 1969;44(8):1203–4. 10.1104/pp.44.8.1203.
48. Kowsalya K, Halka J, Anand M, Sahayarayan JJ, Rajkumar R, Arun M. Unraveling the multifaceted role of ethephon in plant physiology: from seed germination to crop maturation and harvesting. J Plant Biochem Biotechnol. 2025;34(3):639–64. 10.1007/s13562-024-00953-6.
49. Suttle JC. Involvement of Ethylene in the Action of the Cotton Defoliant Thidiazuron. Plant Physiol. 1985;78(2):272–6. 10.1104/pp.78.2.272.
50. Xu J, Chen L, Sun H, Wusiman N, Sun W, Li B, et al. Crosstalk between cytokinin and ethylene signaling pathways regulates leaf abscission in cotton in response to chemical defoliants. J Exp Bot. 2019;70(5):1525–38. 10.1093/jxb/erz036.
51. Li F, Wu Q, Liao B, Yu K, Huo Y, Meng L, et al. Thidiazuron Promotes Leaf Abscission by Regulating the Crosstalk Complexities between Ethylene, Auxin, and Cytokinin in Cotton. Int J Mol Sci. 2022;23(5):2696. 10.3390/ijms23052696.
52. Shan X, Li D, Qu R. Thidiazuron promotes in vitro regeneration of wheat and barley. Vitro CellDevBiol-Plant. 2000;36(3):207–10. 10.1007/s11627-000-0038-y.
53. Liao B, Li F, Yi F, Du M, Tian X, Li Z. Comparative Physiological and Transcriptomic Mechanisms of Defoliation in Cotton in Response to Thidiazuron versus Ethephon. Int J Mol Sci. 2023;24(8):7590. 10.3390/ijms24087590.
54. Beyer E. Silver Ion: A Potent Antiethylene Agent in Cucumber and Tomato1. HortScience. 1976;11(3):195–6. 10.21273/hortsci.11.3.195.
55. McDaniel BK, Binder BM. Ethylene Receptor 1 (ETR1) Is Sufficient and Has the Predominant Role in Mediating Inhibition of Ethylene Responses by Silver in Arabidopsis thaliana*. J Biol Chem. 2012;287(31):26094–103. 10.1074/jbc.M112.383034.
56. Chang SH, Lu LS, Wang NN, Charng Y, yung. Negative feedback regulation of system-1 ethylene production by the tomato 1-aminocyclopropane-1-carboxylate synthase 6 gene promoter. Plant Sci.

2008;175(1):149–60. 10.1016/j.plantsci.2007.11.004. Ethylene Biology.

57. Noori A, Donnelly T, Colbert J, Cai W, Newman LA, White JC. Exposure of tomato (Lycopersicon esculentum) to silver nanoparticles and silver nitrate: physiological and molecular response. Int J Phytoremediation. 2020;22(1):40–51. 10.1080/15226514.2019.1634000 . PubMed PMID: 31282192.

Figures

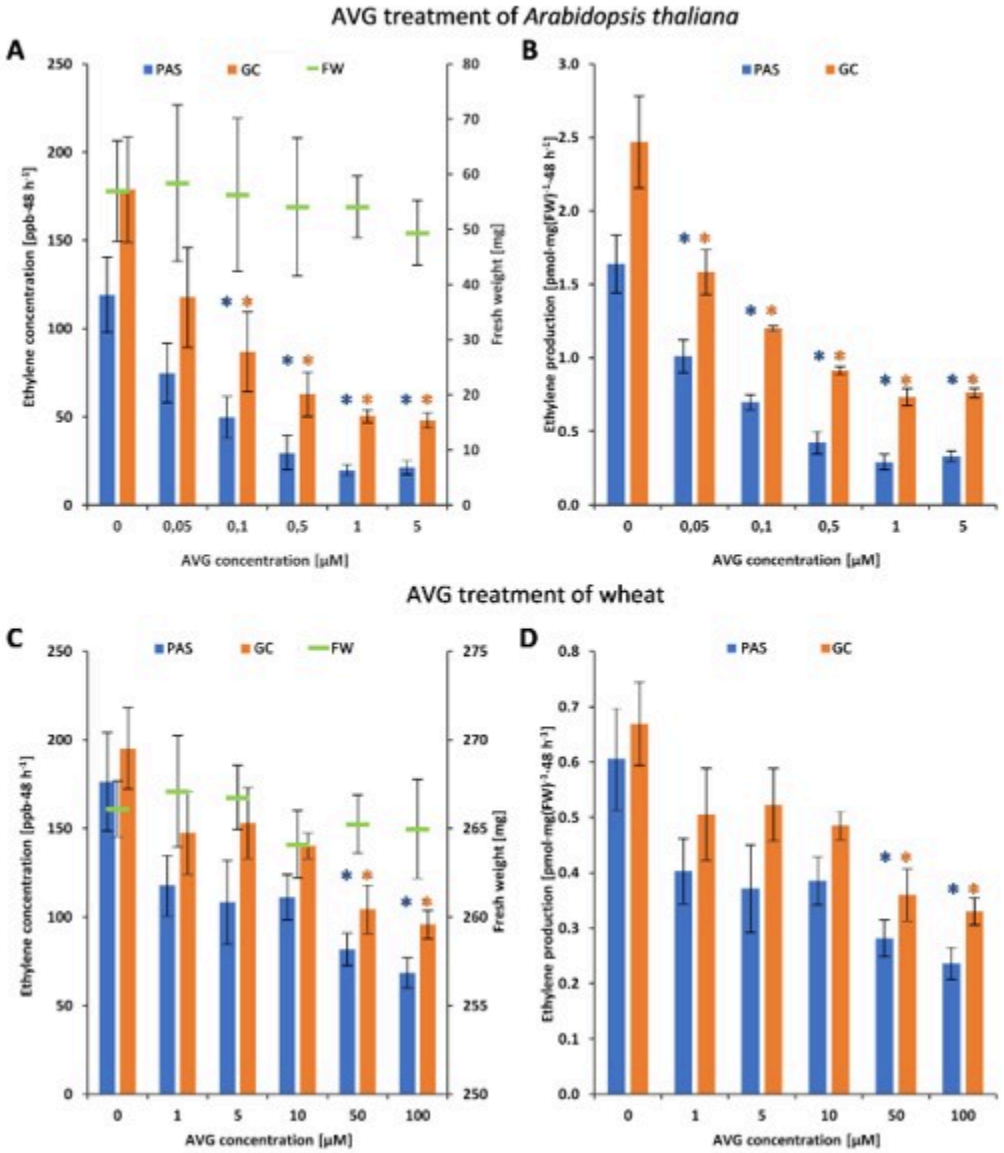


Figure 1

Effects of AVG on ethylene production in Arabidopsis and wheat.

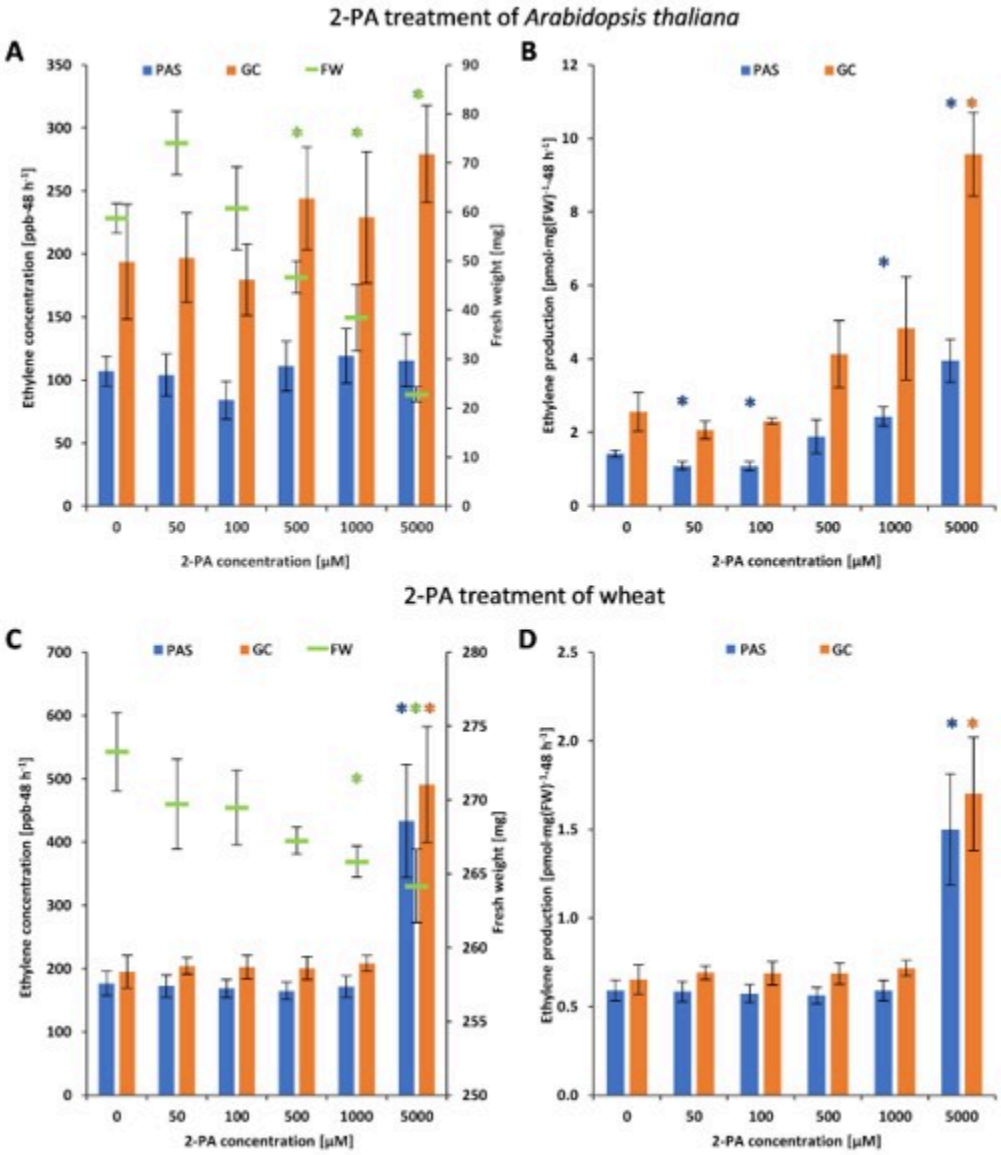


Figure 2

Effects of 2-PA on ethylene production in Arabidopsis and wheat.

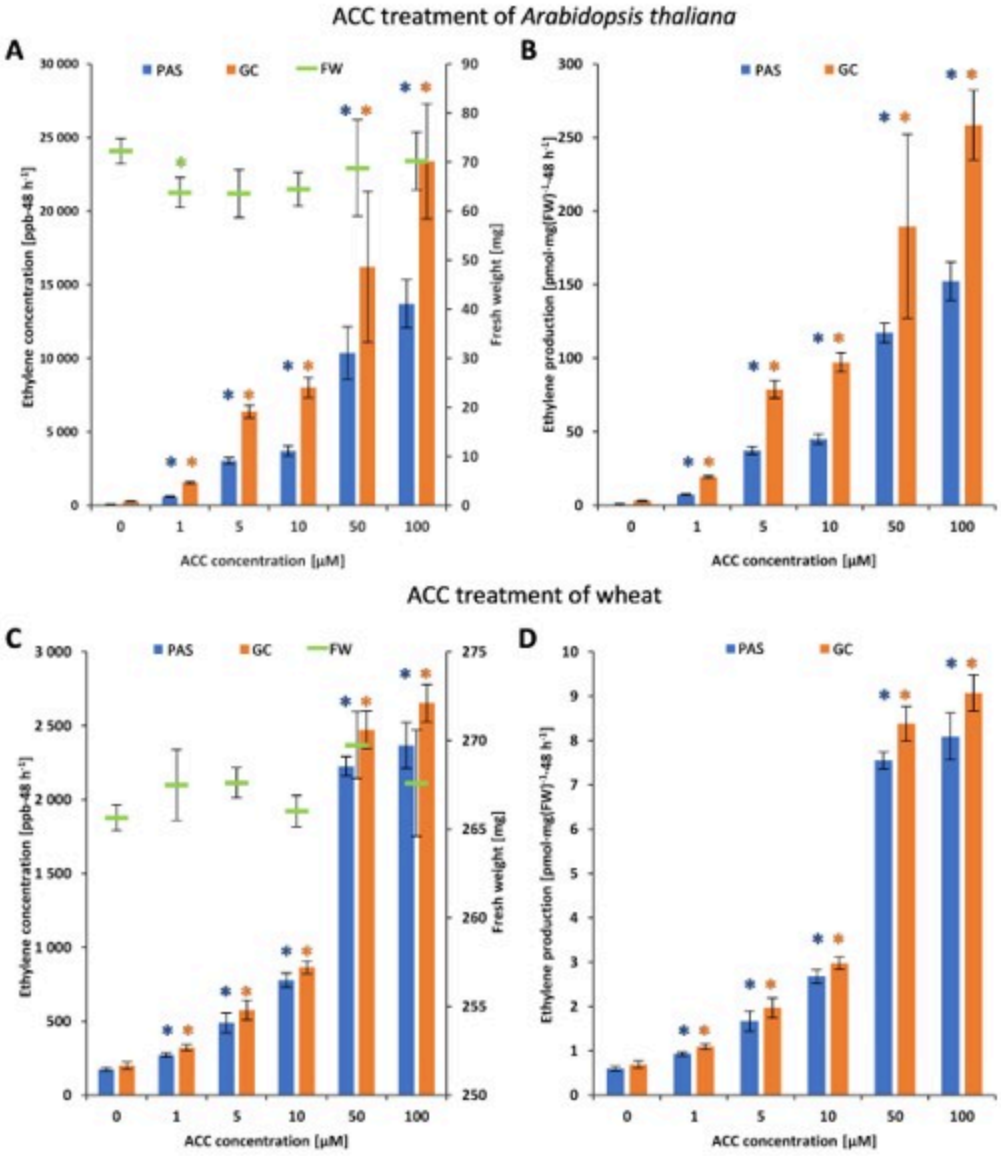


Figure 3

ACC-induced ethylene production in Arabidopsis and wheat.

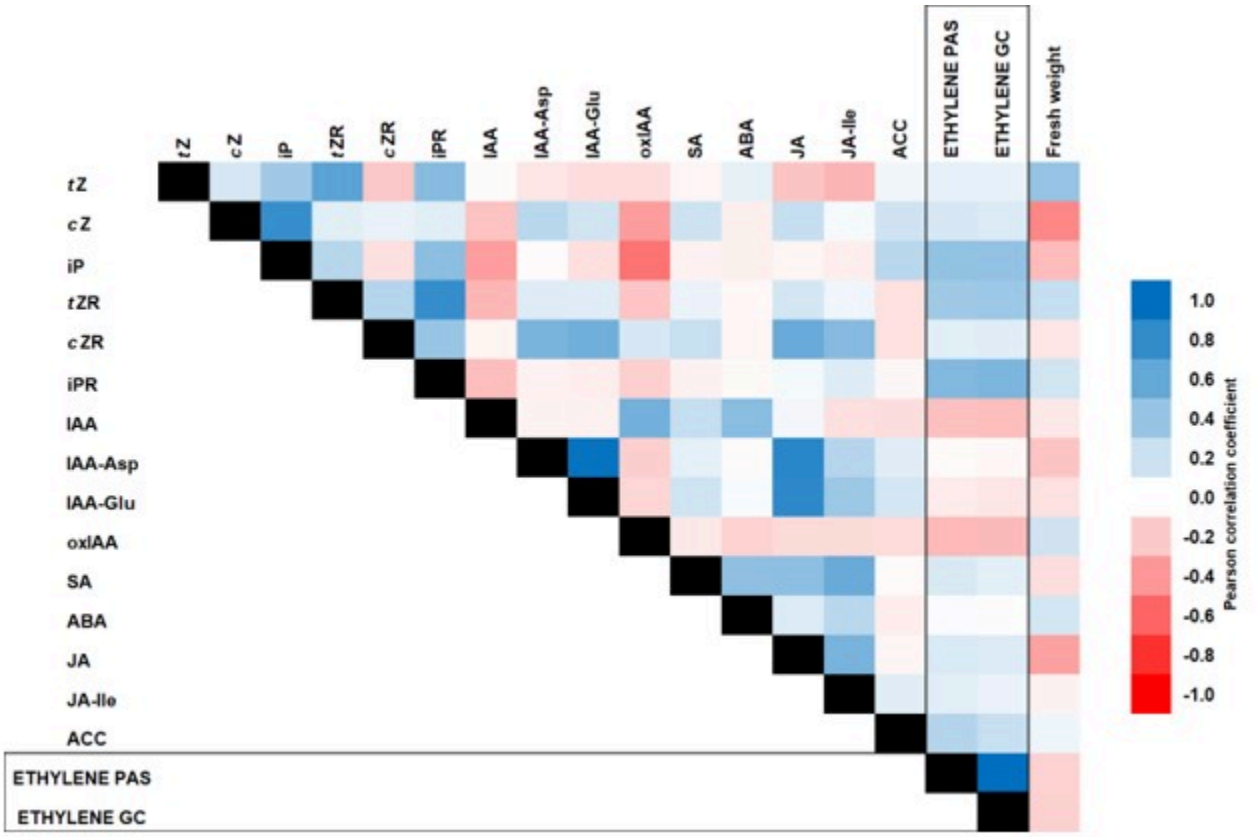


Figure 4

Correlations between ethylene production, ACC, phytohormone contents and fresh weight in Arabidopsis across all treatments

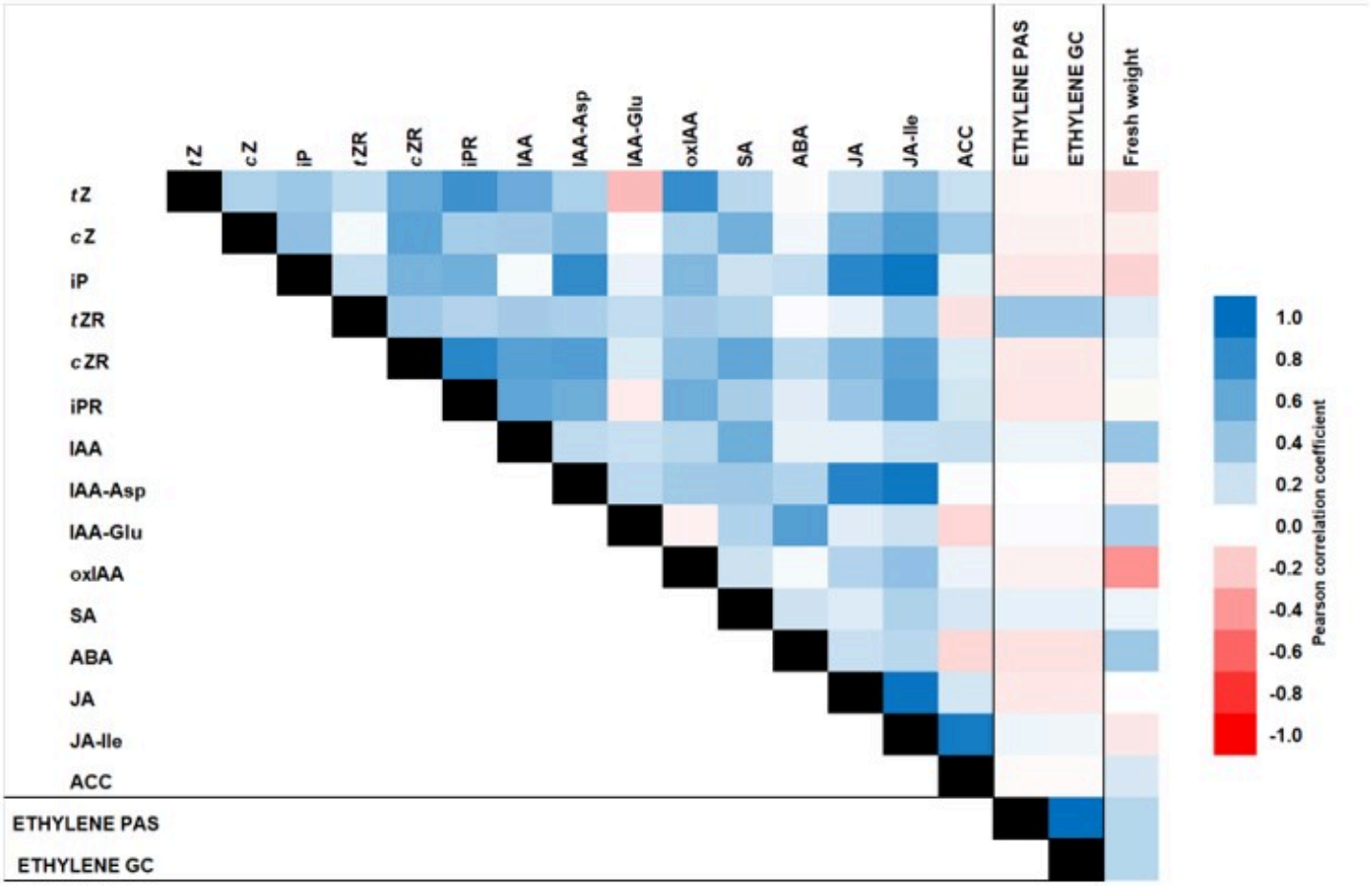


Figure 5

Correlations between ethylene production, ACC, phytohormone contents and fresh weight in wheat across all treatments

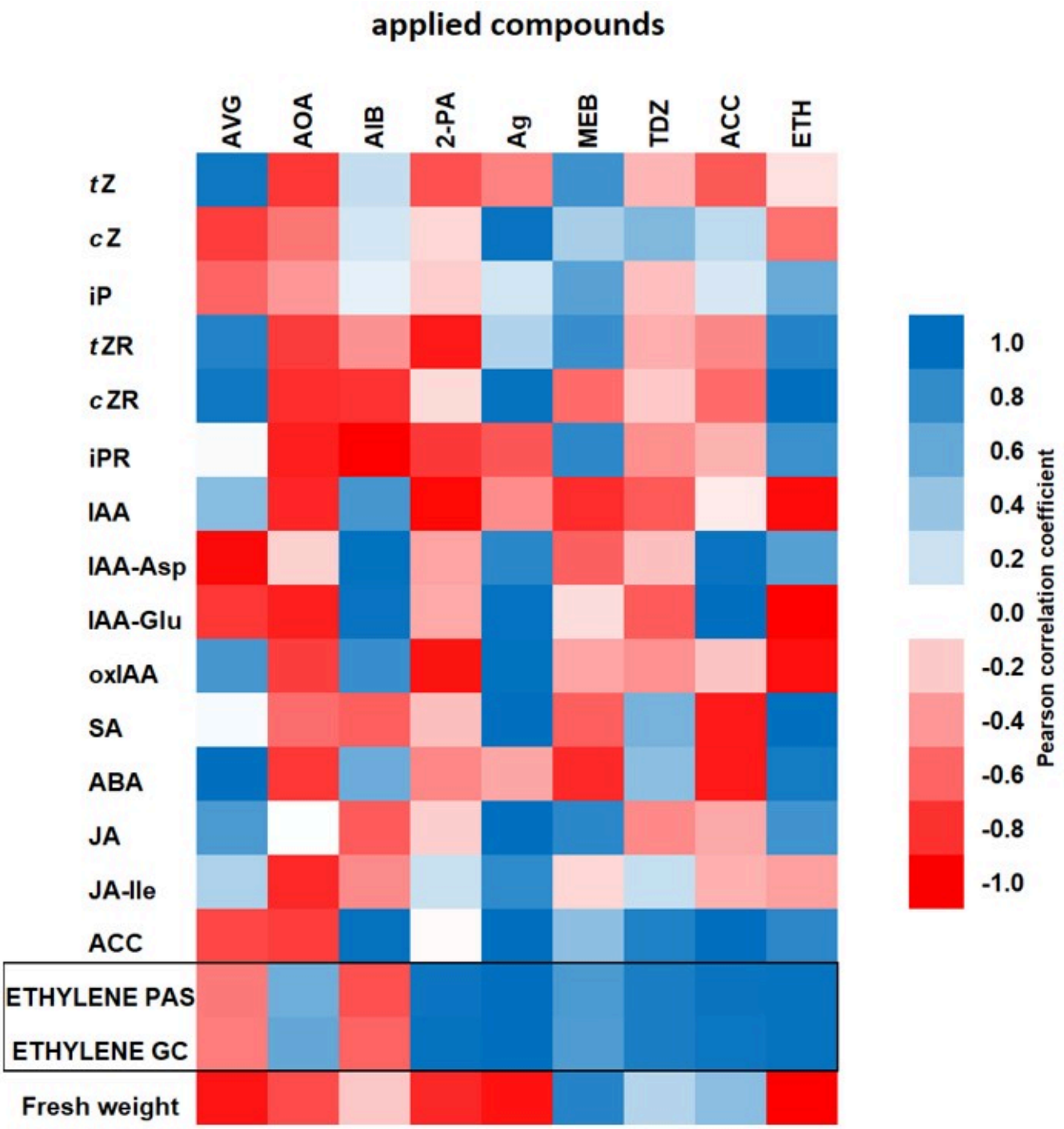


Figure 6

Correlations between applied treatment doses and phytohormone contents in Arabidopsis.

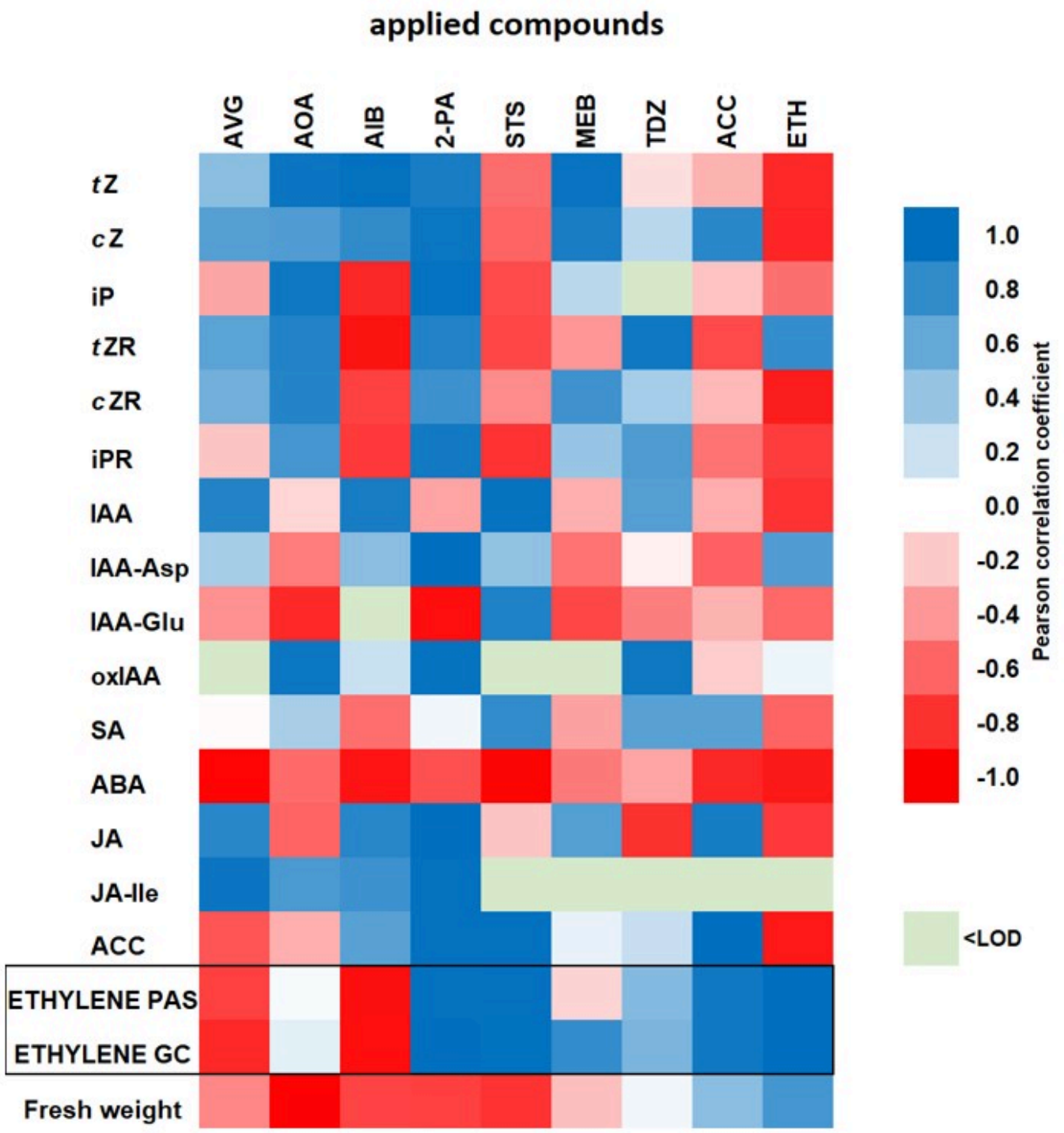


Figure 7

Correlations between applied treatment doses and phytohormone contents in wheat.

Supplementary Files

This is a list of supplementary files associated with this preprint. Click to download.

- Additonalfile11wheatcorrelation.xlsx

- Additonalfile10Atcorrelation.xlsx
- Additonalfile3wheatdata.xlsx
- Additonalfile2Atdata.xlsx
- Additionalfile1linearrange.xlsx
- Additonalfile6ETH.tif
- Additonalfile7TDZ.tif
- Additonalfile8STS.tif
- Additonalfile4AOA.tif
- Additonalfile5AIB.tif
- Additonalfile9MEB.tif
- Supplementaryinformation.docx